The Canadian Mineralogist
Vol. 42, pp. 1443-1464 (2004)

FLUID–MINERAL REACTION IN THE LAKE GEORGE GRANODIORITE, NEW BRUNSWICK, CANADA: IMPLICATIONS FOR Au–W–Mo–Sb MINERALIZATION

Xue-Ming YANG[§] and David R. LENTZ[§]

Department of Geology, University of New Brunswick, P.O. Box 4400, Fredericton, New Brunswick E3B 5A3, Canada

Guoxiang CHI[§]

Department of Geology, University of Regina, Regina, Saskatchewan S4S 0A2, Canada

T. Kurtis KYSER[§]

Department of Geological Sciences and Geological Engineering, Miller Hall, Queen's University,
Kingston, Ontario K7L 3N6, Canada

Abstract

The Early Devonian Lake George granodiorite stock, New Brunswick, Canada, is spatially and temporally associated with early W–Mo–Au and later Au–Sbmineralization. The former mine was the largest antimony producer in North America until the mid-1990s. On the basis of fluid-inclusion analyses, multiple generations of fluids evidently interacted with the granodiorite, with the dominant fluids approximated by the system H_2O–NaCl–CO_2–CH_4. Additional components of the fluid, S–Ca–Fe–K–Mg–Mn, reflect fluid–rock reaction and partial re-equilibration among the rock-forming minerals (*i.e.*, plagioclase, orthoclase, biotite, and hornblende) in the granodiorite. The CO_2-bearing inclusions (Type 1) have a relatively low salinity, ranging from 0 to 15 wt.% equiv. NaCl (ave. 4 wt.%), and most homogenize to the CO_2 phase at temperatures of 200 to 470°C. Inclusions that homogenize to the aqueous phase do so over a narrower range of temperatures (250–350°C). Fluid pressures were probably 740 to 2210 bars for Type-1 inclusions. Aqueous liquid + vapor (Type 2) and aqueous liquid + vapor + halite or sylvite (Type 3) inclusions are recorded as well. Type-2 inclusions show a broader range of temperatures of homogenization (mostly to the aqueous phase), from 150 to 580°C, with a salinity between 2 and 19 wt.% equiv. NaCl. The stable isotope compositions of the rock-forming minerals in the granodiorite exhibit a disequilibrium relationship, *e.g.,* either $\delta^{18}O_{\text{K-feldspar}} > \delta^{18}O_{\text{quartz}}$, $\delta^{18}O_{\text{plagioclase}} > \delta^{18}O_{\text{quartz}}$, or $\delta^{18}O_{\text{plagioclase}} > \delta^{18}O_{\text{K-feldspar}}$. The whole-rock $\delta^{18}O$ values range from 9.4 to 10.7‰, consistent with derivation by contamination by ^{18}O-rich sources. Values of $\delta D_{\text{biotite}}$ range from –75 to –64‰. The bulk fluids entrapped in quartz phenocrysts have δD values of –40.2 ± 5.5‰, consistent with those of the fluids in equilibrium with biotite at temperatures between 350 and 480°C. The similarities among the fluid compositions in the granodiorite, Au–W–Mo quartz–carbonate veinlets and stockworks, and the large Sb veins, suggest that they are genetically related. These fluids are interpreted to be mainly derived from progressive exsolution of volatiles from the cooling magmas at depth, although the CO_2–CH_4-bearing fluids were derived from the intrusion by wall-rock hybridization and skarn-forming reactions and later interaction with groundwater. These CO_2–CH_4-bearing fluids may have reacted with the granodioritic magma to lower its redox conditions, as reflected by a low magnetic susceptibility (ave. 6×10^{-5} SI). Together with the petrochemical features, fluid composition and T–P characteristics in the Lake George granodiorite and associated W–Mo–Au–Sb deposit share many similarities with other reduced I-type granitic-intrusion-related gold systems.

Keywords: fluid inclusions, oxygen isotopes, hydrogen isotopes, carbonic fluids, mineral–fluid interaction, gold mineralization, intrusion-related gold systems, granodiorite, Lake George, New Brunswick, Canadian Appalachians.

Sommaire

Le pluton granodioritique de Lake George, au Nouveau-Brunswick, d'âge dévonien précoce, est associé dans le temps et l'espace à un épisode précoce de minéralisation W–Mo–Au, et ensuite, une minéralisation Au–Sb. La mine de Lake George était le plus important producteur d'antimoine en Amérique du Nord jusqu'au milieu des années 1990. A la lumière des résultats d'analyse des inclusions fluides, de multiples générations de fluides ont de toute évidence réagi avec la granodiorite, les fluides prédominants se rapprochant du système H_2O–NaCl–CO_2–CH_4. Des composants additionnels de la phase fluide, S–Ca–Fe–K–Mg–Mn, résultent des réactions impliquant fluide et roche hôte et d'un ré-équilibrage partiel parmi les minéraux (*i.e.*, plagioclase, orthoclase, biotite, et hornblende) de la granodiorite. Les inclusions à CO_2 (type 1) possèdent une salinité relativement faible,

---

[§] *E-mail addresses*: m0qm4@unb.ca, dlentz@unb.ca, guoxiang.chi@uregina.ca, kyser@geol.queensu.ca

entre 0 et 15% equiv. NaCl (4% en moyenne, base pondérale), et la plupart s'homogénisent à la phase CO_2 à une température entre 200 et 470°C. Les inclusions qui s'homogénisent à la phase aqueuse le font sur un intervalle de températures plus restreint (250–350°C). Les pressions sur la phase fluide étaient probablement entre 740 et 2210 bars pour les inclusions de type 1. Des inclusions de liquide aqueux + vapeur (type 2) et liquide aqueux + vapeur + halite ou sylvite (type 3) sont aussi présentes. Les inclusions de type 2 font preuve d'un plus grand intervalle d'homogénéisation (surtout à la phase aqueuse), de 150 à 580°C, avec une salinité entre 2 et 19% equiv. NaCl (poids). Les compositions des minéraux des roches encaissantes, du point de vue des isotopes stables, montrent des signes de déséquilibre, par exemple, soit $\delta^{18}O_{K\text{-feldspar}} > \delta^{18}O_{quartz}$, $\delta^{18}O_{plagioclase} > \delta^{18}O_{quartz}$, ou $\delta^{18}O_{plagioclase} > \delta^{18}O_{K\text{-feldspar}}$. Les valeurs $\delta^{18}O$ des roches totales vont de 9.4 à 10.7‰, ce qui concorde avec une dérivation par contamination de sources enrichies en ^{18}O. Les valeurs de $\delta D_{biotite}$ vont de –75 à –64‰. Les fluides piégés dans les phénocristaux de quartz ont des valeurs globales de δD de –40.2 ± 5.5‰, conformes à celles de fluides en équilibre avec la biotite à des températures entre 350 et 480°C. Les ressemblances parmi les compositions de fluides dans la granodiorite, les veinules et stockwerks à quartz–carbonate et Au–W–Mo, et les veines plus volumineuses à Sb, mènent à l'hypothèse qu'ils sont tous génétiquement liés. Ces fluides auraient surtout été dérivés par exsolution progressive de composants volatils à partir de magmas en profondeur, quoique les fluides porteurs de CO_2–CH_4 sont plutôt dérivés par réactions d'hybridisation et de formation de skarns aux dépens des roches encaissantes, et d'une interaction tardive avec les eaux souterraines. Ces fluides à CO_2–CH_4 pourraient avoir réagi avec le magma granodioritique pour abaisser sa fugacité d'oxygène, comme le témoigne la faible susceptibilité magnétique des roches (en moyenne, 6×10^{-5} SI). Considérées avec les propriétés pétrochimiques, la composition des fluides et les caratéristiques en termes de T et P de la granodiorite de Lake George et du gisement W–Mo–Au–Sb associé montrent plusieurs ressemblances avec d'autres systèmes aurifères associés à des massifs intrusifs granitiques réduits de type I.

(Traduit par la Rédaction)

Mots-clés: inclusions fluides, isotopes d'oxygène, isotopes d'hydrogène, fluides carboniques, interaction minéral–fluide, minéralisation aurifère, système aurifère lié à une intrusion, granodiorite, Lake George, Nouveau-Brunswick, Appalaches canadiennes.

INTRODUCTION

The Lake George antimony vein deposit is located in York County, New Brunswick (Fig. 1a). Formerly the largest Sb producer in North America, the quartz–Sb veins are spatially and temporally associated with earlier W–Mo mineralization related to an unexposed Early Devonian granodiorite stock (Seal *et al.* 1987, 1988, Procyshyn & Morrissy 1990, Caron 1996, Lentz *et al.* 2002a, Yang *et al.* 2002a, b). Recent assessment of the deposit indicates that Au anomalies are widespread in drill cores around the property (Morrissy 1991a), and ore-grade zones (up to 11.7 g/t Au) are locally developed (Morrissy 1991b, Lentz *et al.* 2002a). The occurrence of Au-bearing quartz–carbonate veinlets and stockworks associated with W–Mo mineralization within the granodiorite stock and the proximal metamorphic aureole strongly suggests that Au mineralization is related to the hydrothermal system associated with the intrusion (Seal *et al.* 1988, Lentz *et al.* 2002a, Yang *et al.* 2002b). Elsewhere in the world, gold mineralization in granitic domains has been documented to be mainly related to metaluminous, subalkaline intrusions of intermediate to felsic composition, which span the boundary between reduced ilmenite and oxidized magnetite series, in continental tectonic settings well inboard of convergent plate boundaries (Thompson *et al.* 1999, Lang *et al.* 2000, Rowins 2000, Lang & Baker 2001, Groves *et al.* 2003). In a preliminary study of the petrochemical attributes of the Lake George granodiorite, Yang *et al.* (2002a) suggested that it is broadly similar to those of gold-associated granitic suites elsewhere. This Early Devonian granodiorite stock (U–Pb zircon age of 412 ± 2 Ma; M.J. McLeod, pers. commun., 2002) may have formed by partial melting of amphibolitic rocks in the lower crust in a volcanic arc. It is genetically linked through fractional crystallization to the Hawkshaw granitic suite (U–Pb titanite age of 411 ± 1 Ma, Whalen 1993), a major phase of the adjacent multiphase Pokiok Batholith (Fig. 1a; Yang *et al.* 2002a). Whalen (1993) noted that the Hawkshaw granite differs slightly from the Lake George granodiorite in that it does not contain hornblende, indicative of its more evolved nature.

A petrological study of the Lake George granodiorite shows that the major rock-forming minerals (*i.e.,* plagioclase, K-feldspar, biotite) appear disturbed and partially reset by subsolidus, late-stage hydrothermal processes (Yang *et al.* 2002b). As pointed out by Martin (1988), the rock-forming minerals in fresh-looking granitic rocks mostly represent the intact pseudomorphs of magmatic phases due to interaction with various fluids. The relationship between the hydrothermal fluids that interacted with the granodiorite stock and those responsible for W–Mo–Au–Sb mineralization remains to be investigated. Fluid inclusions preserved in the stibnite–quartz veins, W–Mo–Au-bearing quartz–carbonate veinlets and stockworks, and the granodiorite may provide important clues as to their genetic relationship. In this study, we focus on the attributes of the fluid phase trapped in the granodiorite and the oxygen and hydrogen isotope compositions of its rock-forming minerals, which are then compared to the characteristics of fluids in the deposits that were documented in previous inves-

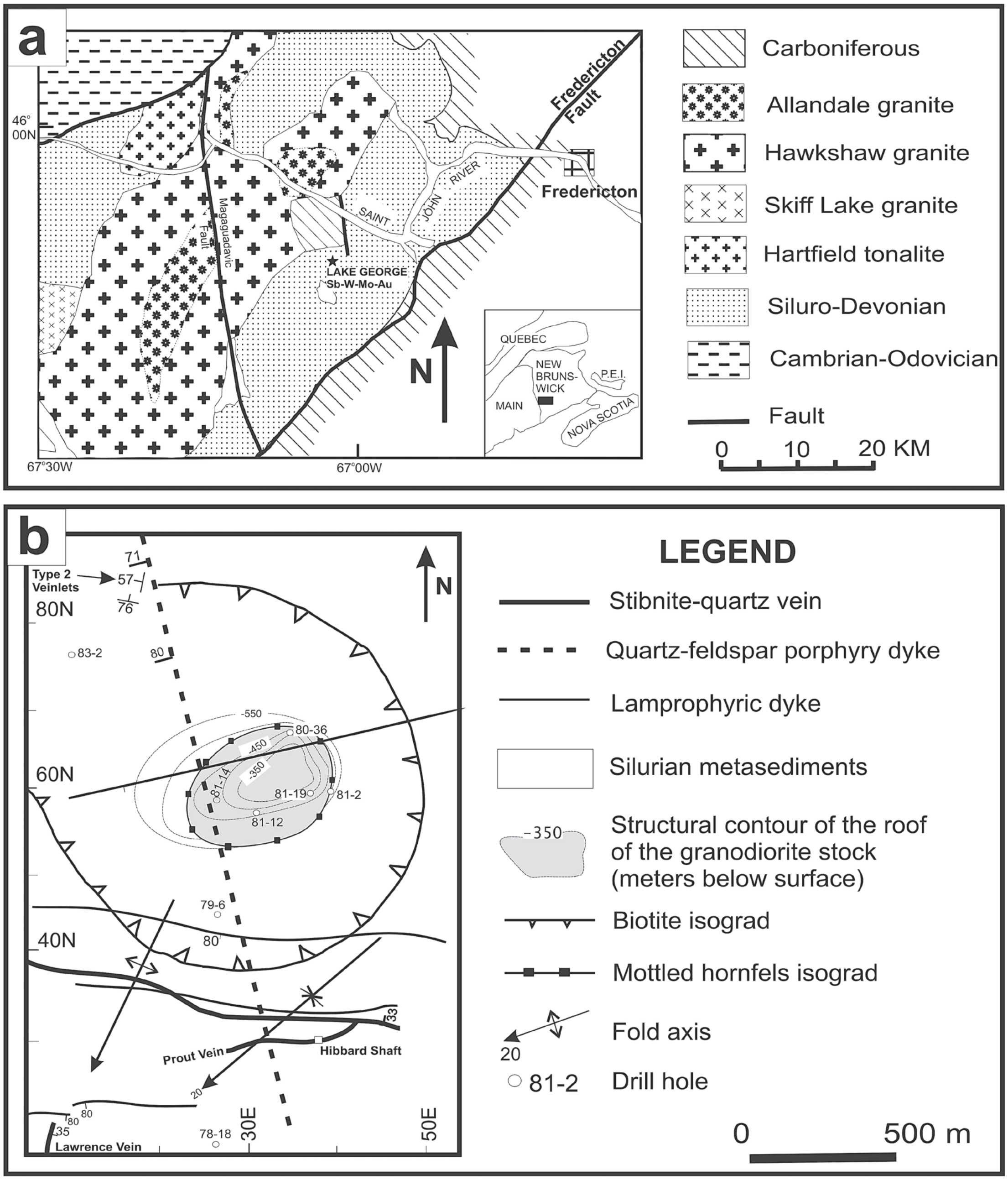

FIG. 1. (a) Location and general geology of the Lake George and Pokiok area, New Brunswick (modified after Procyshyn & Morrissy 1990, McLeod *et al.* 1994). (b) Schematic geological map of the Lake George mine site (modified after Seal *et al.* 1987, Procyshyn & Morrissy 1990). The location of the Lake George granodiorite stock is depicted as structural contours on its upper contact (in meters below the surface). Note the concentric disposition of the biotite and mottled hornfels isograds about the stock.

tigations (Scratch *et al.* 1984, Seal *et al.* 1987, 1988). These new data on fluid inclusions and stable isotopes, together with such data obtained by Chi (2002), provide support for the hypothesis that the recently discovered gold occurrences in southwestern New Brunswick are typical of deposits related to reduced I-type granitic intrusions.

General Geological Setting

Lower Silurian, locally calcareous or marly turbiditic sedimentary rocks (Seal *et al.* 1987, 1988, Caron 1996) of the Kingsclear Group (Fyffe & Fricker 1987) comprise the host rocks to the Lake George deposit (Fig. 1b). These rocks are regionally metamorphosed to the greenschist facies and tightly folded into upright to steeply northwest-dipping, northeast-trending, doubly plunging anticlines and synclines with an axial planar cleavage (Caron 1996). The overall trend of units in the Kingsclear Group parallels the southern margin of the syntectonic to late tectonic Early Devonian granodioritic to granitic Pokiok Batholith (Fig. 1a).

Narrow shoshonitic lamprophyre dykes (414.4 ± 2.4 Ma, Ar–Ar phlogopite, Lentz *et al.* 2004) of calc-alkaline affinity intrude in an overall east–west orientation and generally dip steeply southward (Caron 1996, Lentz *et al.* 2002b). These dykes are intruded by a north–northwest-trending quartz–feldspar porphyry dyke 3–5 m wide (Fig. 1b; see Procyshyn & Morrissy 1990). Intruding the entire package of metasedimentary rocks and dykes is the Lake George granodiorite stock, which has reduced I-type characteristics (Seal *et al.* 1987, 1988, Yang *et al.* 2002a, b). Presently, the cusp of the granodioritic stock at Lake George lies about 350 meters below the present level of erosion, as shown by drilling (Fig. 1b).

Thermal metamorphism associated with the granodiorite stock is superimposed on the regional greenschist-facies metamorphism. Concentric cordierite and biotite isograds delineated by Scratch *et al.* (1984) and Seal *et al.* (1987) outline the symmetrical contact metamorphism, which is overprinted by metasomatism and W–Mo–Au mineralization associated with this high-level stock. The contact-metasomatic mineralized system and the associated granodiorite are subsequently cut by Au-bearing polymetallic veins and the main antimony-bearing systems of veins that contain up to 0.3 g/t gold (Morrissy & Ruitenberg 1980, Procyshyn & Morrissy 1990, Lentz *et al.* 2002a). These features suggest that the thermal metamorphism (formed as a result of heat transferred by fluid associated with intrusion, *cf.* Williams-Jones & Ferreira 1989), contact-metasomatic mineralization, and vein mineralization, all of which are younger than the regional Acadian D1 deformational phase (Seal *et al.* 1987, 1988) and were caused by a complex intrusion-related hydrothermal system. Thus, the characteristics of gold mineralization at Lake George are inconsistent with "orogenic gold deposits" as described by Groves *et al.* (2003), but more similar to their descriptions of intrusion-related gold deposits.

Petrography of the Granodiorite

The fine- to medium-grained porphyritic granodiorite consists of quartz, plagioclase, orthoclase, biotite, hornblende, and accessory minerals such as titanite, zircon, apatite, ilmenite, trace magnetite, and pyrrhotite, pyrite and arsenopyrite (Figs. 2a–f). Phenocrysts, 2–4 mm in size, include subhedral plagioclase with normal zonation (Fig. 2e), euhedral to subhedral hornblende (Figs. 2a, c), and subhedral to anhedral biotite (Figs. 2b, d). Partially embayed quartz phenocrysts are also present (Fig. 3a). A few microperthite grains occur as phenocrysts (Fig. 2f), indicating subsolidus exsolution at temperature lower than 500°C (Tuttle & Bowen 1958). Grains in the groundmass are usually less than 1 mm in size, and are composed of quartz, K-feldspar, plagioclase, biotite, and amphibole. Acicular apatite occurs in plagioclase, biotite, and amphibole phenocrysts. Titanite may occur as a primary phase, but is mostly a product of the alteration of amphibole and biotite, where it is associated with chlorite, magnetite, and calcite. The calcite displays a typical orange-red cathodoluminescence (CL) owing to Mn^{2+} as an activator (Fig. 3i). White mica alteration is ubiquitous in the core of plagioclase crystals and also along cleavages and margins of grains. Chlorite occurs as a common product of alteration of biotite and amphibole. Imaging using the electron-microprobe revealed the presence of muscovite lamellae along cleavage planes within igneous biotite, reflecting partial alteration of this phase.

Textural relations show that apatite and ilmenite were the earliest phases to crystallize from the melt, followed by early hornblende phenocrysts and then by simultaneous crystallization of biotite and plagioclase, and later, by quartz and orthoclase (Yang *et al.* 2002b). Most of the sulfides seem to be hydrothermal in origin, but some ovoid grains of pyrrhotite enclosed in hornblende and biotite may be primary (*i.e.,* magmatic). The granodiorite intrusion has a low magnetic susceptibility (4 to 21×10^{-5} SI, ave. 6×10^{-5} SI), as inferred from measurements on the drill core samples with the Exploranium KT–9 instrument. This indicates a low content of magnetite (Ishihara 1981), consistent with ilmenite as the dominant Ti–Fe oxide in the intrusive body.

The Hawkshaw granite outcrops approximately 3 km northwest of the Lake George Sb deposit (Fig. 1a). It is mainly composed of medium- to coarse-grained, pink K-feldspar porphyritic, biotite granite to granodiorite with minor equigranular biotite granite (Whalen 1993, Whalen *et al.* 1996). The Lake George granodiorite exhibits petrochemical features typical of an I-type granite, derived from partial melting of an arc-like lower continental crust in a volcanic arc or late orogenic environment (Yang *et al.* 2002a), which is consistent with the main batholith (Whalen 1993, Whalen *et al.* 1996). Interestingly, the Lake George granodiorite exhibits features of reduced I-type intrusions (Yang *et al.* 2002a), whereas the Hawkshaw granite belongs to oxidized I-type granitoids, based on mineralogical and petrochemical studies (Whalen 1993, Shabani 1999). Local redox conditions (reduced) may play an important role in gold deposition and associated mineralization.

PETROGRAPHY OF FLUID INCLUSIONS

We studied fluid inclusions in quartz phenocrysts from ten of the least-altered samples of granodiorite taken from drill core of the Lake George granodiorite stock (Fig. 1b) away from the zones of mineralization. Fluid inclusions in acicular apatite enclosed in plagioclase phenocrysts and in late-stage quartz veins cutting the granodiorite also were investigated. The majority of fluid inclusions lying along healed microfractures that cross-cut quartz phenocrysts are considered to be secondary in origin (Figs. 3a, g). However, the relationship between some fluid inclusions and crystal-growth features in quartz phenocrysts cannot be established (Fig. 3h), because the inclusions are irregularly distributed, either occurring in isolation or in clusters; thus, the origin of these inclusions is indeterminate (Roedder 1984, Goldstein & Reynolds 1994). Fluid inclusions in the apatite crystals (Fig. 4e) enclosed in plagioclase and some inclusions in late-stage quartz veins (Figs. 3d–f) are primary in origin, as indicated by their relations to the direction of growth of the host minerals, respectively recording the fluids trapped above (magmatic) and below (possibly postmagmatic) the solidus.

Fluid inclusions were classified on the basis of phase assemblages at room temperature. Three types of fluid inclusions, occurring either as trails along healed fractures, isolated inclusions or as clusters in quartz phenocrysts (Figs. 3a–c, g, Figs. 4a–c, f) from the Lake George granodiorite, are identified and described below.

Type-1 inclusions (aqueous liquid + CO_2 liquid ± CO_2 vapor) (Fig. 4a), comprising 55% of the population of fluid inclusions observed, vary in size (5 to 20 μm), CO_2 total volume-ratios (10 to 100), and shape (negative crystal form, irregular, and elongate). This type of inclusion is characterized by the presence of CO_2 liquid or vapor at room temperature, and in particular by the appearance of the distinct CO_2 liquid and vapor phases during cooling (Fig. 4a). The inconsistency in phase ratios of the inclusions may reflect fluid immiscibility (*i.e.,* CO_2 effervescence) during entrapment.

Type-2 inclusions (aqueous liquid + vapor) (Fig. 4b) are ubiquitous, both in phenocrystic and matrix quartz from the granodiorite. Type-2 inclusions in phenocrystic quartz are variable in size (5 to 14 μm), shape (negative crystal form, irregular, elongate), and vapor proportions (10–60%), and commonly occur along healed fractures. However, some of them also occur in planes or clusters with Type-1 inclusions (Fig. 4f). Type-2 inclusions constitute about 40% of the population of fluid inclusions observed.

Type-3 inclusions (aqueous liquid + vapor + halite or sylvite) (Fig. 4c) are relatively less abundant compared to Type-1 and Type-2 inclusions, constituting only 5% of the population of inclusions observed. Vapor : total fluid ratios in such inclusions are commonly constant, within a range of 20 to 25%. They usually occur as isolated inclusions, although some of the Type-3 inclusions coexist with Type-2 inclusions along the same plane.

In late-stage quartz veins *ca.* 1 mm in width (Figs. 3d–f) that cut the granodiorite, Type-2 inclusions are dominant (Fig. 4d), Type-1 inclusions are minor, and Type-3 inclusions are absent. Type-2 fluid inclusions were also found in apatite (Fig. 4e) enclosed in plagioclase phenocrysts, and these inclusions must predate those inclusions trapped in the quartz phenocrysts and vein quartz.

It is not uncommon for Type-1 and Type-2 fluid inclusions to occur in the same quartz phenocryst, within the same planes or clusters. Also, they show a fairly consistent ratio of phases (Fig. 4f), suggesting that any post-entrapment modification was complete before the nucleation of additional phases. The relative timing of different types of fluid inclusions in the same quartz phenocryst is generally difficult to determine, although trails of most Type-2 inclusions were observed to cut clusters of randomly distributed Type-1 inclusions. Inclusions in the quartz veins may be later than those in the quartz phenocrysts, although they are similar in phase relations to some of the Type 2 inclusions in the phenocrysts. The general sequence of fluid evolution recorded in the Lake George granodiorite is: Type 2 inclusions in apatite → (?) Type 3 inclusions in quartz phenocrysts → Type 1 + Type 2 inclusions in quartz phenocrysts → Type 2 ± Type 1 inclusions in quartz veins. The presence of multiple types and generations of fluid inclusions reflects the complexity of the hydrothermal activity related to the sequential downward crystallization of the Lake George granodiorite stock, with continual fluid evolution from that cooling vapor-saturated magma system at depth.

MICROTHERMOMETRY RESULTS

All microthermometric measurements were performed on a USGS-style heating–freezing stage (made by Fluid Inc., USA) located at the University of New Brunswick, except for a few of measurements carried out at the Quebec Geoscience Centre of the Geological Survey of Canada, also on a USGS-style heating–freezing stage. The accuracy and precision of the measurements of melting and partial homogenization of carbonic phases are estimated to be about ±0.2°C, whereas those of the temperatures of final homogenization are around ±1°C. Fluid composition and T–P conditions were esti-

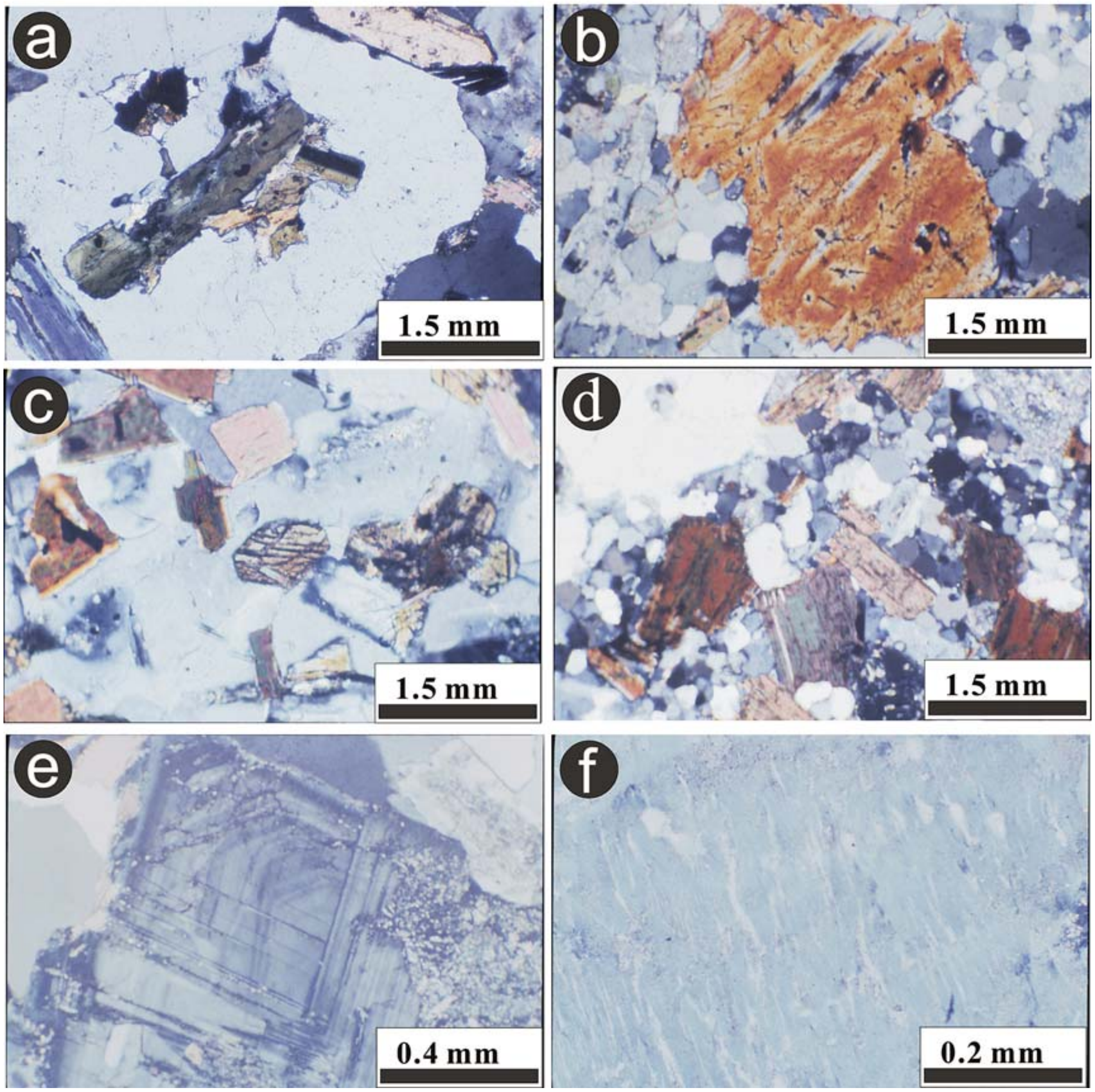

FIG. 2. Photomicrographs illustrating the mineralogy and texture of the Lake George granodiorite. (a) Euhedral hornblende and biotite enclosed by orthoclase; at upper right corner, euhedral titanite partly enclosed in plagioclase (sample LG83–2–2461), cross-polarized light (XPL). (b) Subhedral phenocryst of biotite in fine-grained felsic groundmass consisting of quartz, orthoclase, plagioclase, and opaque phases (sample LG81–12–1567), XPL. (c) Seriate to porphyritic texture, euhedral hornblende enclosed by plagioclase (sample LG81–19–1351), XPL. (d) Seriate to porphyritic texture, subhedral to anhedral biotite, and anhedral ilmenite (and other opaque phases) (sample LG81–14–1886), XPL. (e) Plagioclase phenocryst with normal zoning and polysynthetic twinning as well as pericline lamellae; at the lower right corner, another grain of plagioclase is partially replaced by white mica (sample LG83–2–1995), XPL. (f) Orthoclase with irregular fine lamellae of albite (sample LG83–2–1995), XPL.

mated by using the microthermometric data and the computer program MacFlinCor (Brown & Hagemann 1994). The microthermometric results are summarized in Table 1 and Figures 5 and 6.

Type-1 carbonic fluid inclusions in phenocrystic quartz are the most abundant. Melting temperatures of CO_2 ($T_{m\ CO2}$) vary from –58.0 to –56.6°C (ave. = –57.3°C) (Fig. 5a), with a few as low as –65.6°C. The CO_2 melting data indicate that some of the carbonic inclusions may contain significant CH_4 or N_2, although the clathrate melting temperatures ($T_{m\ clath}$) above 10°C suggest the presence of CH_4 (Shepherd *et al.* 1985). Values of $T_{m\ clath}$ range from 1° to 13°C (ave. = 9°C) (Fig. 5b). Homogenization temperatures of liquid CO_2 (T_{hCO2}) range from 5° to 28°C (ave. = 19°C), but a few measurements record lower values of between –4 and –8°C) (Fig. 5c). Salinities of the carbonic fluid inclusions, calculated from gas clathrate melting temperatures, range from 0 to 15 wt.% equiv. NaCl [ave. = 4 ± 3.3 (1σ) wt.%, *n* = 40: Shepherd *et al.* 1985, Parry 1986], but most are below 6 wt.%. Most of the carbonic inclusions homogenize to the CO_2 phase, although some homogenize to the aqueous phase. Temperatures of final homogenization (T_h) range from 200 to 470°C (Fig. 5d), although those that homogenize to the aqueous phase show a relatively narrow range (250–350°C). Values of T_h for Type-1 fluid inclusions are fairly consistent in a given quartz phenocryst, and show a similar range for those that homogenize to the carbonic phase and aqueous phase, suggesting that these inclusions were trapped from an effervescing fluid system. Consequently, T_h values are assumed to be equal to the entrapment tem-

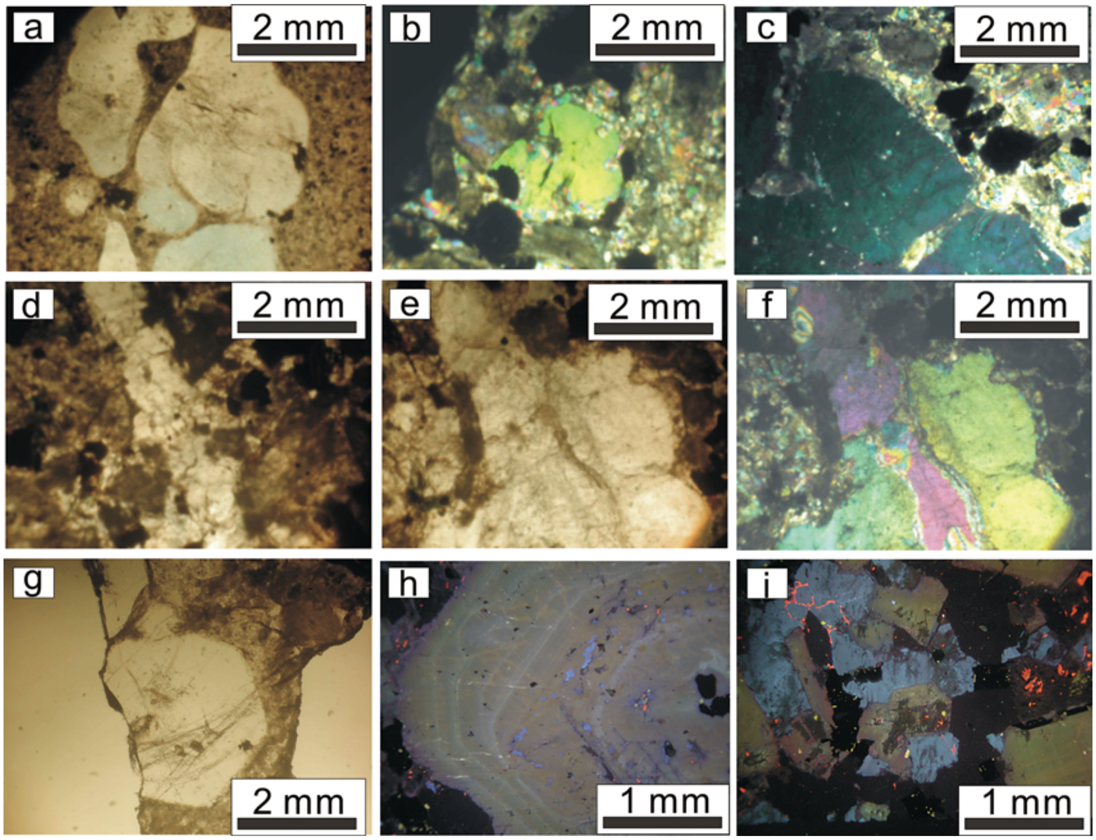

FIG. 3. Photomicrographs of typical phenocrysts of quartz containing abundant secondary fluid inclusions from the Lake George granodiorite, as well as a quartz vein cutting the host granodiorite. (a) Quartz phenocryst in the granodiorite porphyry, whose groundmass is very fine grained and shows features attributed to quenching (sample LG78–18–1190), plane-polarized light (PPL). (b) Quartz phenocryst coexisting with opaque minerals (pyrite, pyrrhotite) (sample LG81–12–1567), XPL. (c) Quartz phenocryst in the granodiorite porphyry; its groundmass is very fine-grained, showing features attributed to quenching, secondary opaque minerals associated with white mica and carbonates (sample LG81–2–1791), XPL. (d) A quartz vein 1 mm wide (late magmatic or postmagmatic) cuts the granodiorite (sample LG80–36–1647), PPL. (e) A quartz vein 1 mm wide (late magmatic or postmagmatic) cuts the granodiorite. Note that it cuts across a quartz phenocryst in the granodiorite (sample LG80–36–1647(2)), PPL. (f) The same view as (e), but with XPL. (g) Abundant secondary fluid inclusions distributed along healed microfractures in a quartz phenocryst (sample LG81–12–1567), PPL. (h) Cathodoluminescence (CL) photograph of a quartz phenocryst showing primary growth-induced zoning, with patches of orange-red-luminescent calcite (secondary) (sample LG81–14–1291). (i) CL photograph showing orange-red-luminescent calcite (secondary) replacing K-feldspar (blue) and biotite (dark) (sample LG81–14–1291).

TABLE 1. FLUID-INCLUSION MICROTHERMOMETRIC DATA FOR THE LAKE GEORGE GRANODIORITE, SOUTHERN NEW BRUNSWICK

Sample no.	Host mineral*	*n*	$T_{m\,CO2}$ °C	$T_{m\,ice}$ °C	$T_{m\,clath}$ °C	$T_{h\,CO2}$ °C	Salinity wt.% NaCl equiv.	T_h °C
LG78-18-1190	Qtz T2	3		-3.8			6.2	265 to 270
LG79-6-617	Qtz T1	2	-57.2 to -56.9			17.8 to 18.1 L		
	Qtz T2	4		-7.8 to -7.2		10.9 to 11.5		160 to 218
LG80-36-1647	Qtz T1	9	-57.6 to -56.6		6.5 to 11.5	4.2 to 25.5 L	0.0 to 6.3	254 to 371
	Qtz T2	3		-7.6 to -0.5			0.9 to 11.2	117 to 165
	VQ T1	4	-65.6 to -56.7		9.3 to 11.2	6.9 to 16.2 L	0.7 to 5.2	208 to 263
	VQ T2	2		-14.9 to -9.0			9.1 to 18.6	201 to 222
LG81-2-1791	Qtz T1	2	-57.2 to -56.8		11.3	15.5 to 21.4 L		300 to 314
LG81-12-1567	Qtz T1	29	-57.8 to -56.6		3.7 to 11.8	14.0 to 26.6 L	0.0 to 13.8	210 to 387
	Qtz T2	14		-15.7 to -1.6			2.7 to 19.2	234 to 401
LG81-14-1291	Qtz T1	5	-57.4 to -56.6		7.6 to 10.4	-8.3 to 11.8 L	4.5	260 to 275
	Qtz T2	4						394 to 412
	Qtz T3	2			264.9 to 270.0[a]		35.7 to 36.0	291 to 293
LG81-14-1886	Qtz T1	3	-57.8 to -57.1		8.6	18.3 to 20.5 V	1.6	407 to 470
	Qtz T2	3		-14.5 to -1.4			2.5 to 18.3	169 to 515
	Ap T2	3		-11			15.0	570 to 581
LG81-19-1351	Qtz T2	3		-9.0 to -2.9			9.3 to 12.9	237 to 331
	VQ T2	4		-4.6 to -1.4			2.4 to 7.3	118 to 214
LG83-2-1995	Qtz T1	9	-57.4 to 56.7		7.9 - 11.2	22.8 to 27.4 L	0.5 to 4.0	324 to 385
	Qtz T2	2		-7.5 to -7.9			11.1 to 11.6	271 to 340
LG83-2-2461	Qtz T1	7	-58.0 to -56.7		7.2 to 10.6	20.0 to 27.2 L	0.0 to 5.4	306 to 413
	Qtz T2	4		-10.5 to -1.8			3.1 to 14.5	116 to 348
	Qtz T2	3		-10.7 to -3.8			6.2 to 14.7	182 to 275

$T_{m\,CO2}$ denotes melting temperature of CO_2, $T_{m\,ice}$ is temperature of final melting of ice, $T_{m\,clath}$ represents the melting temperature of clathrate, $T_{h\,CO2}$ is the temperature of homogenization of CO_2 phases, and T_h is the temperature of final homogenization. a: temperature of halite dissolution. Qtz: quartz. *n*: number of samples. * and type of inclusion (T1: Type 1, T2: Type 2, VQ: vein quartz).

peratures (T_t) (Roedder 1984). On the basis of the method described by Diamond (2001), fluid pressures estimated from isochores of the vapor-rich inclusions (CO_2/total = 100%, no visible aqueous phase could be identified), with temperatures approximated by those of liquid-rich inclusions (250–350°C) range from 740 to 2210 bars (Fig. 5e). These pressures correspond to lithostatic depths of approximately 2.8 to 8.4 km, with a rock density of 2.7 g/cm^3 being used for calculation (Shepherd *et al.* 1985).

Type-2 aqueous fluid inclusions are ubiquitous, both in phenocrystic and matrix quartz from the granodiorite. Because the size of inclusions in the matrix is relatively small (<5 μm), the present study mainly focused on inclusions in quartz phenocrysts. These fluid inclusions in phenocrystic quartz are variable in size (5 to 14 μm), shape (negative crystal form, irregular, elongate), and vapor proportions (10–60%). Temperatures of last melting of ice ($T_{m\,ice}$) (–15.7 to –1.5°C) (Fig. 6a) indicate salinities of 19.2 to 2.5 wt.% equiv. NaCl (Fig. 6b), using the equation of Bodnar & Vityk (1994). Most of the inclusions homogenize to the liquid phase over a broad range of temperatures (T_h), from 150 to 580°C. Some inclusions homogenize to the vapor phase (Fig. 6c). We note that fracture-controlled fluid inclusions in phenocrystic quartz are characterized by low salinity (<3.5 wt.% equiv. NaCl) and low T_h (110–270°C), values that are similar to those in quartz veins cutting the host rock. Fluid inclusions in apatite (Fig. 4e) show a consistent range of T_h (570–581°C), with a salinity of 15 wt.% equiv. NaCl.

Type-3 halite–sylvite-bearing fluid inclusions are relatively rare; only a few inclusions were investigated. The dissolution temperature (T_s) of the daughter mineral ranges from 264.9 to 270.0°C, corresponding to salinities of 35.7 to 36.0 wt.% equiv. NaCl (Bodnar & Vityk 1994). The temperatures of final homogenization (to liquid) (varying from 291.3 to 292.5°C) of Type-3 inclusions are slightly higher than T_s. Fluid pressure of Type-3 inclusions is below 1 kbar (*cf.* Bodnar 2003).

ANALYSIS OF DECREPITATE MOUNDS

Analysis of decrepitate mounds using scanning electron microscopy (SEM) or electron-probe micro-analyzer (EPMA) has proved to be a relatively simple and reliable semiquantitative method to evaluate fluid composition (Hayes *et al.* 1988, Savard & Chi 1998, Kontak *et al.* 2001, Kontak 2002). Decrepitate mounds hosted by quartz from the granodiorite and a narrow quartz vein (1 mm wide) cutting the granodiorite were analyzed with a JEOL JSM–6400 SEM, LINK–eXL X-ray micro-analyzer, at conditions of 15 kV and 1.5 nA. The techniques used in this study are slightly different from

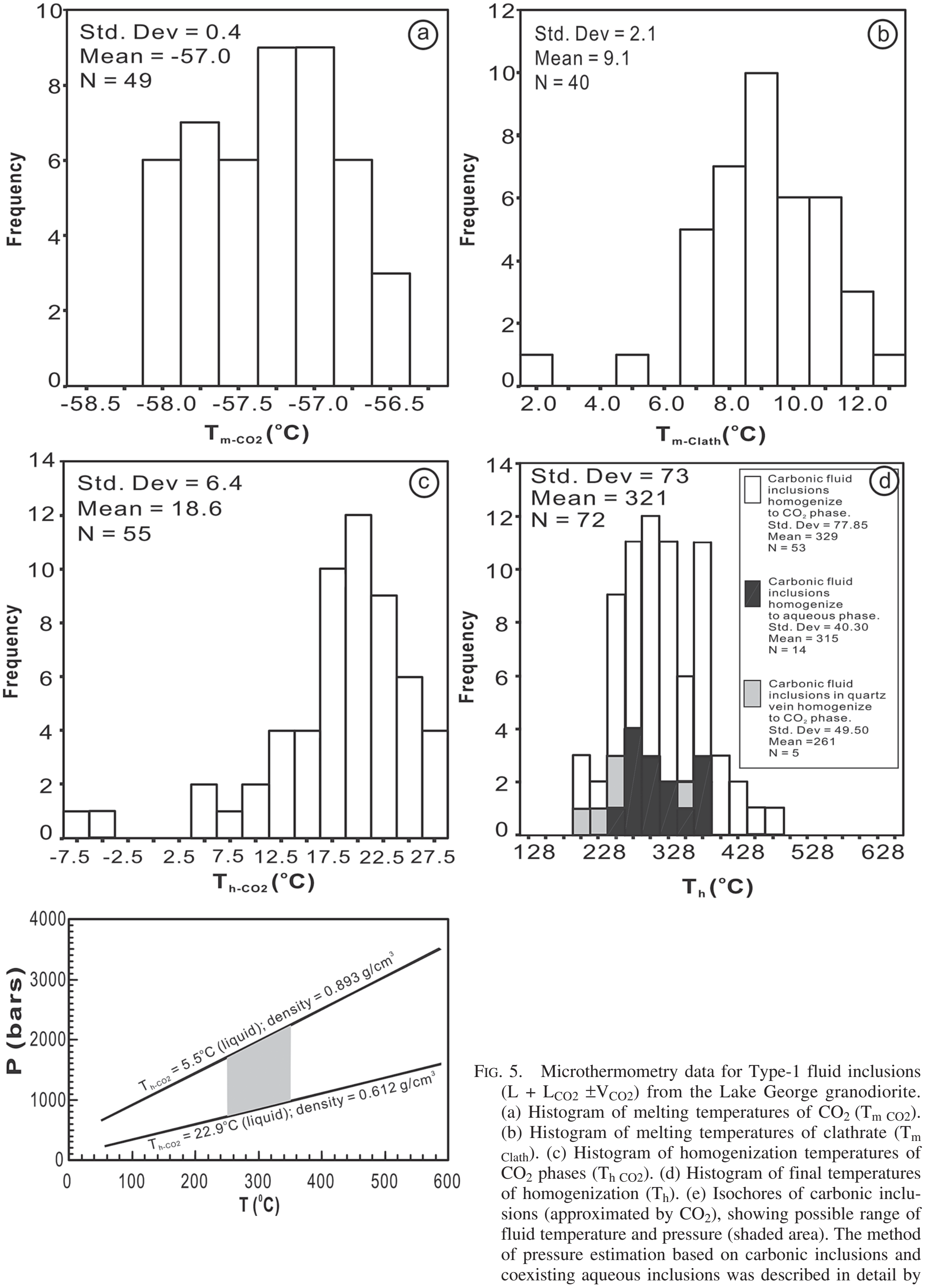

FIG. 5. Microthermometry data for Type-1 fluid inclusions ($L + L_{CO2} \pm V_{CO2}$) from the Lake George granodiorite. (a) Histogram of melting temperatures of CO_2 ($T_{m\ CO2}$). (b) Histogram of melting temperatures of clathrate ($T_{m\ Clath}$). (c) Histogram of homogenization temperatures of CO_2 phases ($T_{h\ CO2}$). (d) Histogram of final temperatures of homogenization (T_h). (e) Isochores of carbonic inclusions (approximated by CO_2), showing possible range of fluid temperature and pressure (shaded area). The method of pressure estimation based on carbonic inclusions and coexisting aqueous inclusions was described in detail by Diamond (2001).

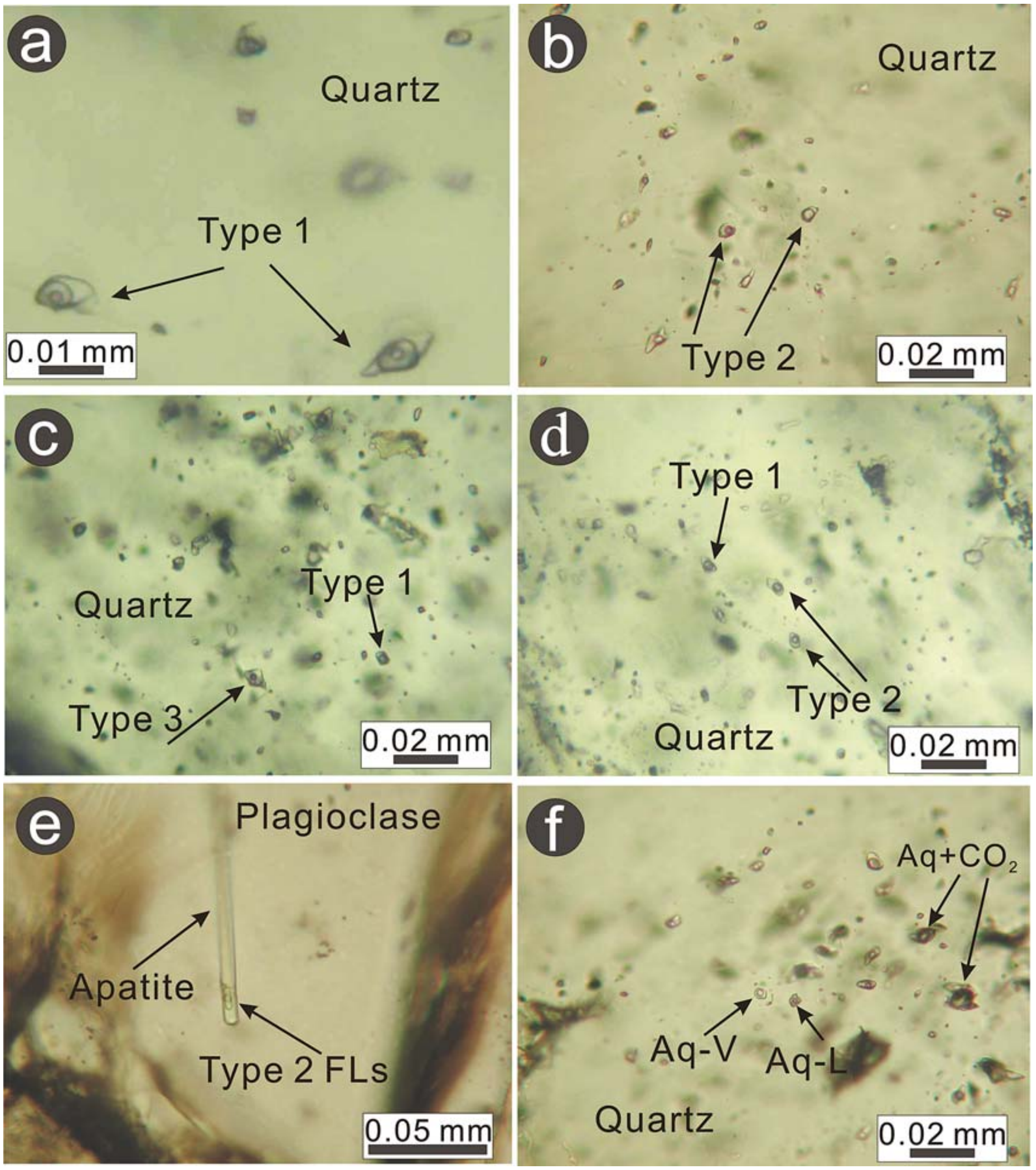

FIG. 4. Petrography of fluid inclusions and host minerals from the Lake George granodiorite. (a) Type-1 fluid inclusions consist of three phases: liquid CO_2 (L_{CO2}) + vapor CO_2 (V_{CO2}) + aqueous liquid (L), at room temperature (18°C in this case), hosted in quartz phenocryst (sample LG80–36–1647). (b) Type-2 fluid inclusions are composed of two phases: L + vapor (V), hosted in quartz phenocryst. Note that values of the ratio V/(L +V) are variable (sample LG83–2–1995). (c) Type-3 fluid inclusions comprise three phases: L + V + S (halite or sylvite) (sample LG81–14–1291). (d) Type-2 fluid inclusions are dominant in the quartz vein (Fig. 3d) that cuts the host granodiorite, and minor Type-1 inclusions also occur (sample LG80–36–1647). (e) Type-2 inclusion hosted in apatite that is enclosed in plagioclase from the Lake George granodiorite; V/(V + L) = 30% (sample LG81–14–1886). (f) Type-1 and type-2 fluid inclusions occur in the same crystal of quartz (sample LG83–2–1995).

those adopted by previous investigators in that microthermometric measurements of fluid inclusions were first determined on a USGS heating–freezing stage, and then the samples were transferred to a muffle furnace for 30 minutes to decrepitate the fluid inclusions at 700°C. Various shapes of the mounds (*i.e.*, irregular, elongate to tabular) were found (Fig. 7). The decrepitate mounds of Type-1 carbonic fluid inclusions are characterized by Na–Ca–Fe–K–Mg–Mn mixtures, whereas those from Type-2 fluid are similar, but do not contain Mn. Appreciable sulfur was detected in the decrepitate mounds of both types of fluid inclusions; the fluids thus contain notable amounts of sulfur in addition to chlorine.

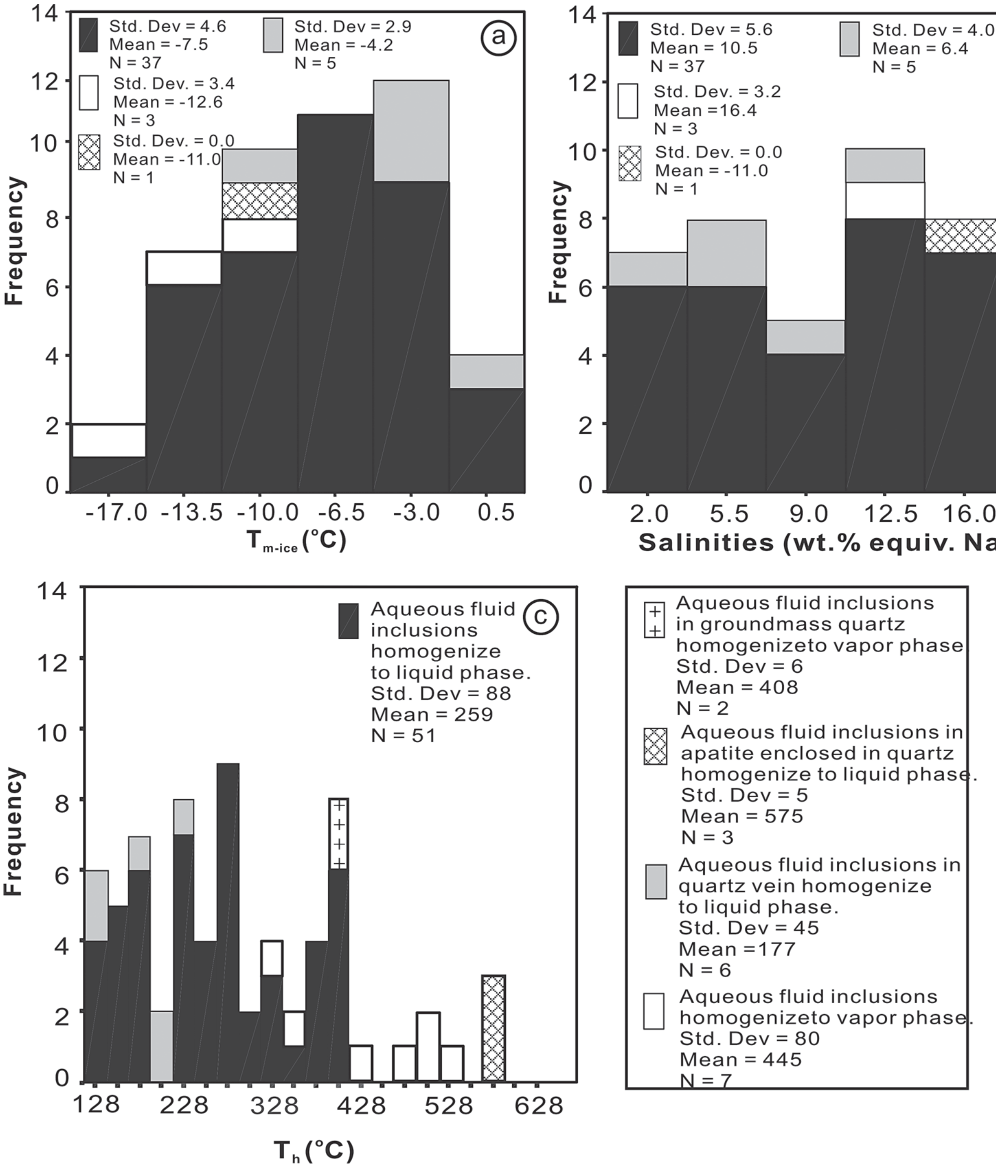

FIG. 6. Microthermometry data for Type-2 fluid inclusions (L + V) from the Lake George granodiorite. (a) Histogram of temperatures of final melting of ice ($T_{m\,ice}$). (b) Histogram of salinities (equiv. wt.% NaCl). (c) Histogram of temperatures of final homogenization (T_h). The symbols in (a) and (b) are the same as those in (c), which represent different behaviors of the fluid inclusions during heating or different host minerals (*i.e.,* quartz and apatite) and textural relations. See text for details.

OXYGEN AND HYDROGEN ISOTOPE COMPOSITIONS

Hand-picked separates of quartz, K-feldspar, plagioclase, and biotite from six granodiorite samples were analyzed for oxygen isotopes, with hydrogen isotopes being analyzed for biotite and bulk fluid inclusions extracted from the quartz phenocrysts. Hornblende obtained from one sample (LG81–14–1886) also was analyzed for oxygen and hydrogen isotopes. Detailed analytical methods were described by Kyser *et al.* (1999). Estimated errors on reported δ values relative to V–SMOW are ±0.2‰ for oxygen and ±3‰ for hydrogen isotopes at the 1σ level. The results are presented in Table 2, together with calculated temperatures for mineral pairs assuming oxygen isotope equilibrium between phases.

In most samples, ^{18}O enrichment in the rock-forming minerals exhibits an abnormal, disequilibrium sequence, *e.g.,* either $\delta^{18}O_{\text{K-feldspar}} > \delta^{18}O_{\text{quartz}}$, $\delta^{18}O_{\text{plagioclase}} > \delta^{18}O_{\text{quartz}}$, or $\delta^{18}O_{\text{plagioclase}} > \delta^{18}O_{\text{K-feldspar}}$ (Table 2). Only one sample (LG81–14–1886) appears to have normal ^{18}O fractionation among the minerals (*e.g.,* quartz > K-feldspar > plagioclase > biotite > hornblende; *cf.* Taylor 1978). The calculated temperatures for the mineral pairs are inconsistent with one another, *e.g.,* $T_{\text{quartz–K-feldspar}}$ 998°C, $T_{\text{quartz–plagioclase}}$ 836°C, and $T_{\text{quartz–biotite}}$ 514°C (Table 2). These features suggest that magmatic equilibration among the minerals in the Lake George granodiorite was disturbed by late-stage hydrothermal fluids, consistent with petrological investigations (Yang *et al.* 2002b). Notably, feldspar and biotite are apparently enriched in ^{18}O during fluid–rock reaction, elevated by 2 to 4‰ (Fig. 8), in comparison with primary (*i.e.,* magmatic) quartz–feldspar (*ca.* 2‰) and quartz–biotite (ca. 6‰) fractionation. In contrast, $\delta^{18}O$ values of quartz remain relatively constant (9.2 to 10.6‰), consistent

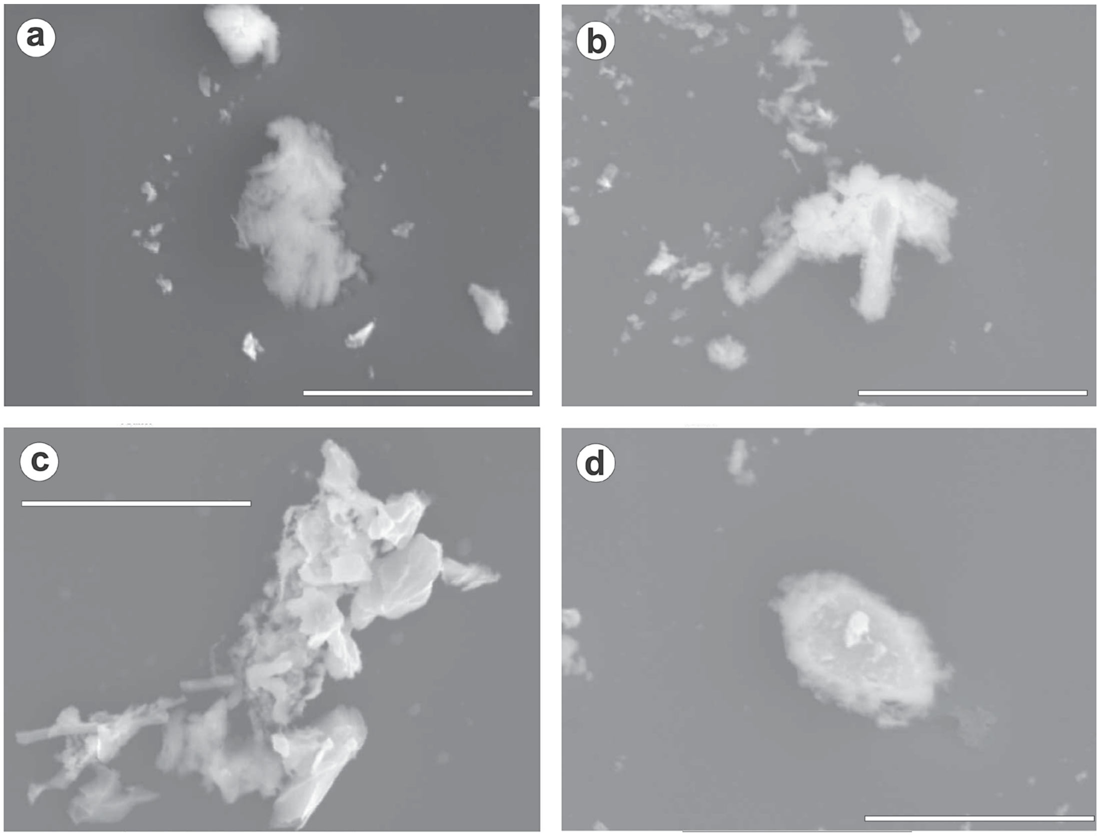

FIG. 7. Secondary electron images of decrepitate mounds hosted by quartz from the Lake George granodiorite. (a) Very fine-grained mixture of Na–Ca–Fe–K–Mg–Mn salts (sample LG83–2–1995). (b) Very fine-grained irregular to elongate mixture Na–Ca–Fe–K–Mg–Mn salts (sample LG80–36–1647). (c) Irregular and elongate mixture of Na–K–Ca–Fe–Mg compounds (sample LG81–14–1291). (d) Tabular Ca–Fe–K–Mg–Mn mixture (sample LG80–36–1647). Note that all these mounds contain an amount of sulfur. The scale bars are 10 µm in length.

with their low relative susceptibility to oxygen isotope exchange with fluid (Longstaffe 1982, Criss & Taylor 1983, Gregory & Criss 1986).

The bulk $\delta^{18}O_{quartz}$ values (Table 2) of the granodiorite samples are estimated to range from 9.4 to 10.7‰ (ave. 10.2‰), based on the mode of the samples and corresponding mineral $\delta^{18}O$ values. Given that the feldspar $\delta^{18}O$ values (Table 2) are not primary, but in fact reflect low-temperature re-equilibration with a hydrothermal fluid, these values represent a maximum for the whole rock. The whole-rock $\delta^{18}O$ values are in the high part of the range for normal granites, and are slightly higher than $\delta^{18}O$ value for the Hawkshaw granite (9.6‰, see Whalen *et al.* 1996). Such high $\delta^{18}O$ values are consistent with derivation by contamination with an ^{18}O-enriched source (Taylor 1978, 1988).

The $\delta D_{biotite}$ values are fairly constant, ranging from –75 to –64‰ (Table 2), similar to those of hypothetical magmatic biotite (Taylor 1974). The bulk fluids entrapped in quartz phenocrysts have higher δD values, –40.2 ± 5.5‰ (Table 2). Such δD values of bulk fluids are consistent with those of the fluids in equilibrium with biotite at temperatures between 350 and 480°C using the fractionation factor for hydrogen isotopes between biotite and H_2O (Suzouki & Epstein 1976). Hornblende has a lower δD value, –106‰, than the biotite and fluids extracts from the quartz phenocrysts.

DISCUSSION

Data on the fluid-inclusion microthermometry presented here suggest the fluid systems that interacted with the Lake George granodiorite may be approximated by

TABLE 2. OXYGEN AND HYDROGEN ISOTOPIC COMPOSITIONS OF ROCK-FORMING MINERALS FROM THE LAKE GEORGE GRANODIORITE, NEW BRUNSWICK

Sample no.	Mineral	$\delta^{18}O$ ‰	δD ‰	$T_{Qtz-Ksp}$ °C	T_{Qtz-Pl} °C	T_{Qtz-Bt} °C
LG81-2-1741	Qtz	10.0	-48			506
	Ksp	11.0				
	Pl	10.3				
	Bt	6.1	-68			
	WR	10.1				
LG81-12-1567	Qtz	10.0	-32			559
	Ksp	12.1				
	Pl	10.7				
	Bt	6.7	-64			
	WR	10.5				
LG81-14-1886	Qtz	10.6	-41	998	836	514
	Ksp	10.0				
	Pl	9.8				
	Bt	6.7	-71			
	Hb	6.5	-106			*514
	WR	9.9				
LG81-19-1351	Qtz	9.5	-38			571
	Ksp	11.9				
	Pl	11.4				
	Bt	6.1	-75			
	WR	10.7				
LG83-2-1995	Qtz	10.5	-38	1284		449
	Ksp	10.1				
	Pl	10.7				
	Bt	5.9	-73			
	WR	10.3				
LG83-2-2461	Qtz	9.2	-44			553
	Ksp	9.3				
	Pl	10.0				
	Bt	5.6	-68			
	WR	9.4				

The O isotope composition of whole rocks is estimated on the basis of the modal proportion of minerals and their O isotope composition. The oxygen isotope geothermometry used in this study: $1000 \ln\alpha_{Qtz-Ksp} = 0.97 \times (10^6 \times T^{-2})$, where T in Kelvin (see Friedman & O'Neil 1977); $1000 \ln\alpha_{Qtz-Pl} = (0.46 + 0.55\beta) \times (10^6 \times T^{-2}) + (0.02 + 0.85\beta)$, $1000 \ln\alpha_{Qtz-Bt} = (2.73 - 0.49\beta) \times (10^6 \times T^{-2}) + (0.85\beta - 0.58)$, and $1000 \ln\alpha_{Qtz-Hb} = (2.64 - 0.49\beta) \times (10^6 \times T^{-2}) + (0.85\beta - 0.28)$, where β is the mole fraction of anorthite in plagioclase (the data are taken from Yang *et al.* 2002b) (see Bottinga & Javoy 1975, Matsuhisa *et al.* 1979). Symbols: Qtz quartz, Ksp K-feldspar, Pl plagioclase, Bt biotite, Hb hornblende, WR whole rock. * T_{Qtz-Hb}.

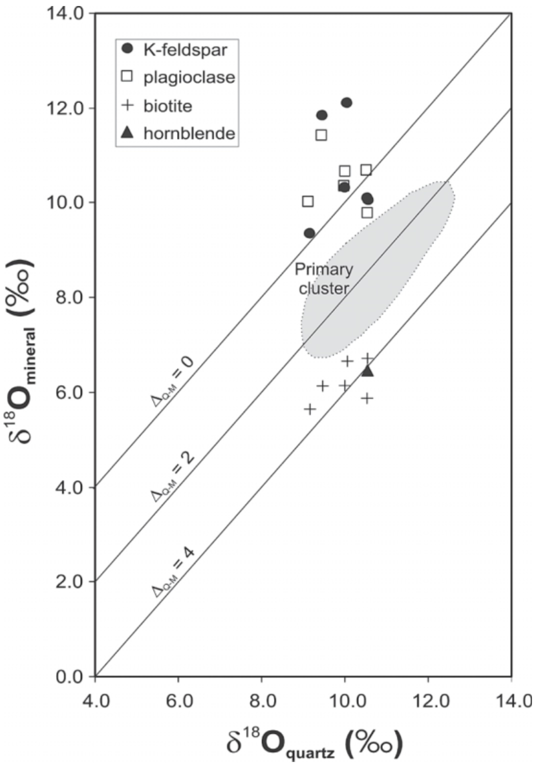

FIG. 8. Values of $\delta^{18}O$ relations in coexisting quartz, feldspar, biotite, and hornblende in the Lake George granodiorite. The primary cluster of granitic samples without hydrothermal alteration has a quartz–feldspar fractionation of 2‰ ($\Delta_{Q-M} = 2$) (Criss & Taylor 1983). Compared to quartz, the $\delta^{18}O$ values of K-feldspar, plagioclase, and biotite are somewhat elevated at about 2 to 4‰, which requires that the fluid that reacted with these minerals was rich in ^{18}O or at low temperature.

the system $H_2O–NaCl–CO_2–CH_4$. This is characteristic, although not diagnostic, of deeper parts of the newly recognized type of intrusion-related gold systems (Thompson *et al.* 1999, Lang & Baker 2001, Baker & Lang 2001, Baker 2002, Chi 2002, Fan *et al.* 2003, Groves *et al.* 2003); aqueous fluid inclusions with variable salinities are documented as well. Late-stage fluids in the quartz veins that cut the host granodiorite are characterized by low-temperature and low-salinity aqueous fluids (of Type 2), although minor CO_2-bearing inclusions also occur. Type-2 inclusions in apatite recorded the highest temperature of homogenization with moderate salinity (15 wt.% equiv. NaCl); they are interpreted to represent a primary magmatic fluid trapped at the early stage of volatile saturation during the magmatic evolution. Type-1 fluid inclusions were not observed in apatite, on the basis of our limited dataset, and less abundant Type-3 inclusions (halite- or sylvite-bearing) may represent the residual fluids of Type 2 in apatite. If a pressure correction is considered for this fluid in apatite (Roedder 1984), then the temperatures of trapping are as high as 770–780°C, which is above the solidus temperature of H_2O-saturated granodiorite (Whitney 1988).

Secondary Type-1 and Type-2 inclusions seem to coexist in phenocrystic quartz, although their relative timing is difficult to determine. If generated simultaneously, they may represent episodic unmixing of a parental aqueous–carbonic fluid. Cooling and decompression may be major causes of immiscibility of CO_2-bearing fluid (Bowers & Helgeson 1983, Frantz *et al.* 1992). However, only Type-2 fluid inclusions, interpreted to be primary magmatic fluid, were found in apatite enclosed in plagioclase, suggesting that this fluid predated those trapped in Type-1 and Type-2 inclusions in the quartz phenocrysts. Trapping of exsolved fluids in the apatite probably occurred during rapid crystallization induced by pressure quenching of the magma. Volatile saturation may start at relatively higher pressures, recorded by the hornblende geobarometer (3–5 kbar), in comparison to the lower pressures inferred for final emplacement of the stock (< 2 kbar), based qualitatively on quenched textures, Ab–Or–Q–H_2O phase equilibria, and contact-metamorphic mineral assemblages (Seal *et al.* 1987, 1988, Yang *et al.* 2002b). Hydrofracturing associated with volatile saturation may be responsible for the pressure-quench phenomena, and a high flux of fluid linked with exocontact-related mineralization around the granodiorite stock. Progressive cooling of the magmas inward to the core of the magma chamber at depth (*cf.* Marsh 1996) may have led to emanations of relatively high-temperature (350-470°C), low-salinity, and CO_2-rich fluids (Type 1), which interacted with the upper part of solidified granodiorite stock and were trapped in the quartz phenocrysts, mainly as secondary inclusions. These fluids were favorable for Au, Sb, W, and Mo partitioning from the granodioritic magma into the fluid (Bowers 1991, Keppler & Wyllie 1991, Frank *et al.* 2002) and resulted in formation of stockwork mineralization within the granodiorite and the contact-metamorphic aureole.

Furthermore, low-salinity (<3.5 wt.% equiv. NaCl) secondary aqueous fluid inclusions in the quartz phenocrysts also are ubiquitous. In addition to the magmatic fluids from depth, these fluids may have interacted with other rock-forming minerals in the granodiorite as well, resulting in partial to complete re-equilibration, as indicated by inconsistency of two-feldspar thermometry (*i.e.*, $T_{Ab} < 500°C$, $T_{An} = 342–1950°C$, $T_{Or} = 350–668°C$), as well as by the large range in halogen fugacity ratios $[\log(f_{HF}/f_{HCl}) = –2 \text{ to } 0$, at 400°C] for fluids in equilibrium with biotite (Yang *et al.* 2002b). Oxygen isotope thermometry also indicates disequilibrium among the rock-forming minerals (Table 2). These low-temperature and low-salinity fluids may be attributed to input of circulating groundwater. However, these fluids are not considered be related to Au mineralization, as they are considerably different both in temperature and salinity from those in quartz from both Sb veins, and gold-bearing W–Mo veinlets and stockworks (Scratch *et al.* 1984, Seal *et al.* 1987, 1988).

Figure 9 shows the relationship of the salinities of fluid inclusions to final temperatures of homogenization for the Lake George granodiorite. No simple correlation can be discerned from the dataset. Multiple generations of fluids thus interacted with the granodiorite, reflecting the complexity of fluid evolution. However, the P and T conditions of entrapment of the fluid inclusions in the granodiorite can be estimated in terms of fluid isochores (Fig. 10) and constraints on either P or T conditions determined with other methods. The broad scenario of fluid evolution recorded in granodiorite may be generalized temporally. Magmatic fluid associated with pressure quenching of the granodiorite stock was trapped in apatite (Type-2 inclusion at P and T conditions of entrapment *ca.* 1.3 kbar, *ca.* 770–780°C); cooling of this fluid may generate hypersaline fluid (Type-3) trapped (secondary) in quartz phenocrysts (≤1 kbar, *ca.* 375°C); below 500–600°C, the upper part of the stock was already solidified, although the downward cooling magma was progressively releasing CO_2-bearing fluids. Rising and cooling of these magmatic fluids resulted in immiscibility to generate Type-1 and Type-2 inclusions, which interacted with the granodiorite stock and were trapped in the quartz phenocrysts, mainly as secondary inclusions (*ca.* 2.2 – 0.7 kbar, *ca.* 250–470°C). Late-stage quartz veins cut the granodiorite, trapping low-salinity and low-T fluids (180–290°C) dominated by Type-2 (but containing minor Type-1) inclusions, which is interpreted as convective groundwater driven by the granodiorite stock.

Comparison with previous fluid-inclusion studies at Lake George

Previous fluid-inclusion studies were focused on the Au-bearing quartz–Sb veins and W–Mo–Au systems of

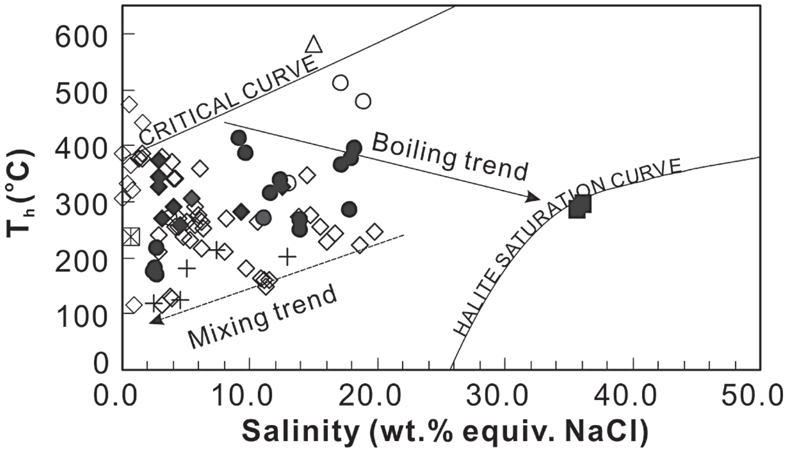

FIG. 9. Relations of the salinities of fluid inclusions to final temperatures of homogenization from the Lake George granodiorite. Boiling and mixing trends are shown for comparison. Solid diamonds (◆) are carbonic inclusions homogenizing into the aqueous phase, open diamonds (◇) represent carbonic inclusions homogenizing into the CO_2 phase, squares with cross (☒) represent carbonic inclusion in quartz vein homogenizing into CO_2 phase, solid circles (●) represent aqueous inclusions that homogenize into the liquid phase, open circles (○) are aqueous inclusions that homogenize into the vapor phase, open triangle (Δ) is the aqueous inclusion in apatite that homogenizes to the vapor phase, crosses (+) denote the aqueous inclusions in quartz vein homogenizing into the liquid phase, and solid squares (■) represent brine inclusions with halite that homogenize to the liquid phase. No apparent track can be defined from the data, reflecting the complexity of fluid activities recorded.

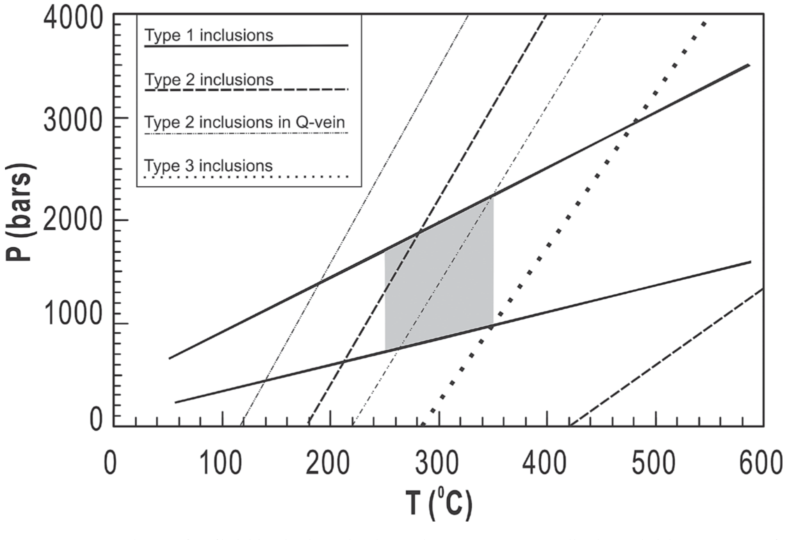

FIG. 10. Isochores for fluid inclusions in the Lake George granodiorite. Fluid pressures of Type-1 inclusions, estimated as described by Diamond (2001), range from 740 to 2210 bars (see texture for details). The pressure (1.3 kbar) of Type-2 inclusions in phenocrystic quartz is assumed to be constrained by the assemblage of metamorphic minerals (Seal *et al.* 1987), so that the entrapment temperatures are between 250° and 595°C; Type-2 inclusions in the quartz veins that cut the granodiorite were entrapped at 180° to 290°C; Type-2 inclusions in apatite may have been trapped at 770–780°C. Type-3 inclusions are entrapped below 1 kbar, so that the maximum temperature of entrapment is 375°C.

veinlets. Three types of fluid inclusions occur in the quartz–Sb vein systems: aqueous liquid–vapor inclusions, aqueous liquid–vapor–halite polyphase inclusions, and CO_2-bearing inclusions (Scratch *et al.* 1984). They determined T_h values to trace the direction of fluid migration, and provided salinity data solely for the halite-bearing inclusions (38–40 wt.% equiv. NaCl). The values of T_h decrease from in excess of 350°C in the deep easterly workings to less than 325°C in the western Adams workings. This represents a gradient of about 25°C in 600 m, implying that the fluids flowed along the vein (fault) systems and follow the gradient of declining temperatures (Scratch *et al.* 1984).

Seal *et al.* (1988) pointed out that the variability in liquid : vapor ratio in inclusions reported by Scratch *et al.* (1984) may have been due to CO_2 effervescence. They estimated that the fluids responsible for quartz–Sb mineralization occurred at *ca.* 1.3 kbar, based on the Sb mineralization closely associated in time with W–Mo(–Au) mineralization that was barometrically well constrained (Seal *et al.* 1987). The salinities of the fluids in the Hibbard Vein (Fig. 1b) were found to range from 1.5 to 18.0 (ave. 8.2) wt.% equiv. NaCl (see Seal *et al.* 1988).

Seal *et al.* (1987, 1988) extensively documented the fluid-inclusion geochemistry in two types of W–Mo veinlets at Lake George: (1) calc-silicate veinlets are dominated by two-phase aqueous inclusions, although three-phase (brine + CO_2-rich liquid + vapor) were locally encountered; (2) quartz–scheelite veinlets are dominated by variable proportions of three-phase (brine + CO_2-rich liquid + vapor), two-phase (CO_2-rich liquid + vapor) and two-phase (brine + vapor) inclusions. Values of T_h for inclusions in the calc-silicate veinlets range from 178 to 384°C, and salinities are 4.1–17.5 wt.% equiv. NaCl (ave. 10.0 wt.%). Values of T_h for inclusions from the quartz–scheelite veinlets entrapped from non-effervescing fluid range from 405 to 350°C, whereas those entrapped from an effervescing fluid range from 350 to 142°C, with salinities of 1.0–19.6 wt.% equiv. NaCl (ave. 6.7 wt.%). The melting temperatures of CO_2 in inclusions from the quartz–scheelite veinlets are between –76 and –56.6°C, suggesting the presence of variable methane (from nil to >45 mole %) in the CO_2-rich phase. The first-melting temperatures of brine in inclusions from both types of veinlets were as low as –50°C, suggesting the presence of dissolved $CaCl_2$ and $MgCl_2$, in addition to NaCl. This is confirmed by analyses of decrepitate mounds discussed above. A confining pressure of 1.3 kbar was estimated for entrapment of the effervescing fluid, assuming that the fluid consists of 6.7 wt.% equiv. NaCl and 17 mole% CO_2 at 350°C (Seal *et al.* 1987, 1988).

The results of previous studies on fluid inclusions from W–Mo–Sb–Au mineralization (Scratch *et al.* 1984, Seal *et al.* 1987, 1988) demonstrate their similarities in phase relations, final homogenization, and salinities with the fluids in quartz phenocrysts from the granodiorite in this study, and thus their genetic linkage. They may be derived from a common hydrothermal system, with the complexity of fluid inclusions recorded in the granodiorite a good indicator for its high potential of mineralization. Interestingly, Sn, W, and Mo deposits associated with granite intrusions have comparable types of fluid inclusion and reduced conditions (Linnen 1998), compared to the data of this study and intrusion-related gold systems.

The source of CO_2

Abundant carbonic fluid inclusions (Type 1) trapped in the Lake George granodiorite may be important with respect to the origin of the various mineralizing systems, in particular gold. The source of this CO_2 is presently enigmatic, although there are several possibilities. Considering the subduction-related petrogenesis of the granodiorite (Yang *et al.* 2002a), three possible origins for the carbonic component of the fluids are considered: (1) subduction-related partial melting of the lower crust or the mantle sources (deep), (2) assimilation, hybridization or skarnification reactions involving sedimentary rocks of the upper crust during emplacement, possibly including local host-rocks (intermediate), and (3) circulation of hydrothermal fluids through local carbonate-bearing and organic-carbon-bearing sedimentary rocks (*e.g.,* Kingsclear Group) during cooling of the intrusion (shallow).

Several east–west-trending, steeply south-dipping narrow Early Devonian lamprophyre dykes occur at the Lake George mine site (Fig. 1b), and many more occur along the southern boundary of the Pokiok Batholith (Seal *et al.* 1987, Caron 1996, Lentz *et al.* 2002b). Emplacement of these dykes seems to immediately precede emplacement of the Lake George granodiorite stock (Lentz *et al.* 2004). They show arc-type geochemical associations (low Ti, Y, Nb, and high U, Th, La, Ce) similar to lamprophyric dykes of calc-alkaline affinity (Lentz *et al.* 2002b), suggesting a mantle-derived component for part of the magmatic evolution in this area. Hence it is plausible that there was a deep source of CO_2 from the mantle incorporated into the granodioritic magma during subduction-related partial melting of the lower crust.

The CO_2-bearing fluids taken up into the intrusion from wall rocks, as a result of hybridization reactions, may be an alternative mechanism for the source of the fluids. Abundant carbonate (up to 40% locally) and black shale within the turbiditic metasedimentary rocks (*i.e.,* the Kingsclear Group, see Caron 1996) may provide a possible source of CO_2 and CH_4 through a series of decarbonation reactions (Seal *et al.* 1987) and hybridization (Lentz 1996). The incorporation of aqueous fluids during metamorphic devolatilization-type reactions usually leads to oxidization of the hornfels along the contact (*cf.* Yardley & Long 1981). The reduced characteristics of the granodiorite may result from its reaction with hydrothermal fluids bearing CO_2–CH_4. These fluids may partly be derived from complex hybridization reactions (see Lentz 1996), and the magmatic sources may provide CO_2-bearing fluids at an earlier stage during evolution of the hydrothermal systems. Fluids exsolved from the cooling granodioritic magma may become more H_2O-rich and saline during saturation and continued decompression (Lowenstern 2001).

Sources of fluids reacting with the granodiorite

Magmatic equilibrium between the rock-forming minerals in the Lake George granodiorite was disturbed chemically (Yang *et al.* 2002b) and isotopically, suggesting that it reacted with late-stage hydrothermal fluids. Examples of these fluids are preserved in healed fractures in quartz phenocrysts, as indicated by the three types of inclusions. In terms of various calibrations of oxygen isotope fractionation between minerals and H_2O, as well as hydrogen isotope fractionation between biotite and H_2O, the stable isotope compositions of the fluids can be deduced from the measured mineral isotopic values, assuming apparent equilibrium temperatures obtained from fluid inclusions in this study. The $\delta^{18}O$ and δD values of fluids reacted with the granodiorite at temperatures between 300 and 600°C range from 3.1 to 10.6‰ and from –60 to –22‰, respectively (Fig. 11), consistent with fluids derived from progressively degassing of magmas at depth.

Three altered samples of granodiorite have $\delta^{18}O$ values of 12.8–15.1‰ (Scratch *et al.* 1984), higher than the values of the least-altered samples presented in this study, suggesting that they were affected by low-temperature fluids. As shown above, very low-temperature (<100°C) fluids recorded in the granodiorite are negligible, although a variable portion of secondary inclusions with low salinity and low to medium T_h do occur; these may represent significant involvement of convective groundwater in the system driven by the granodiorite intrusion.

Local shales have high $\delta^{18}O$ values (16.0–22.4‰, ave. = 18.9 ‰, $n = 3$, Scratch *et al.* 1984), so that any fluid reacted with the shales must have be elevated in $\delta^{18}O$ value. Interestingly, calculated $\delta^{18}O$ and δD com-

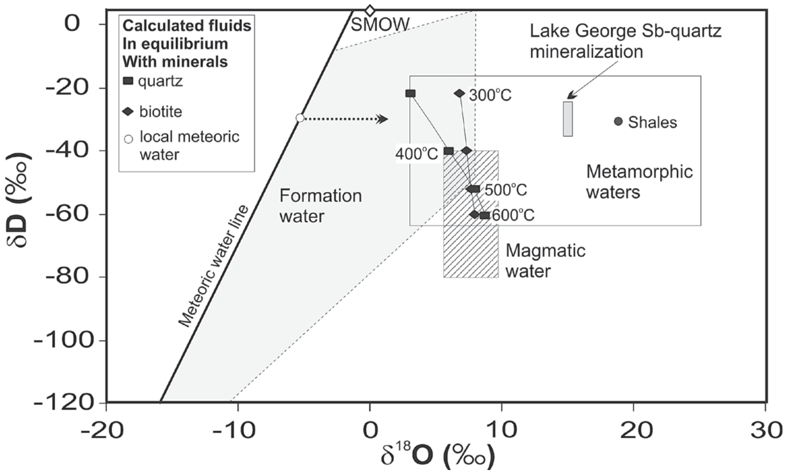

FIG. 11. The stable isotope compositions ($\delta^{18}O$ and δD) of fluids that reacted with the Lake George granodiorite, in comparison with terrestrial fluid reservoirs (modified from Taylor 1974, Rollinson 1993). The evolving tracks of the fluids in equilibrium with the rock-forming minerals at temperatures between 300° and 600°C are shown (see text for detailed explanation); we use the average oxygen isotope value of quartz and biotite as a basis of calculation and use an average hydrogen isotope ratio of the biotite to constrain the fluids reacted with these minerals. The calibration of oxygen isotope fractionation between minerals and H_2O are used: quartz–H_2O (Clayton *et al.* 1972), biotite–H_2O (Bottinga & Javoy 1975, Friedman & O'Neil 1977). Hydrogen isotope fractionation between biotite and H_2O is based on Suzouki & Epstein (1976). The compositions of meteoric water, assumed to be $\delta^{18}O$ = –5‰ and δD = –30‰, are also shown. The data for Cambro-Ordovician shales are from Scratch *et al.* (1984). The field of the Lake George quartz–Sb vein mineralization and related hydrothermal alteration is from Seal *et al.* (1988), who recalculated the original data of Scratch *et al.* (1984).

positions of fluids in equilibrium with the granodiorite are significantly lower than that of the ore fluids responsible for the formation of the Sb–quartz veins, with $\delta^{18}O = 14.4 – 15.5$ ‰, $\delta D = –36 – –24$ ‰ (see Seal *et al.* 1988). This requires addition of ^{18}O from the country rock to the vein fluids. Values of $\delta^{34}S$ in three stibnite samples from Lake George (–5.8, –4.6 and –1.8 ‰) (R. Seal, pers. commun., 2003) also reflect a role of sedimentary sulfur in Sb mineralization.

Genetic considerations

Various episodes of mineralization occurred at Lake George (Figs. 1b, 12), including exocontact Au–W–Mo veinlet and stockwork mineralization (Type I), polymetallic auriferous veins (Type II), and Au-bearing antimony veins (Type III) (Scratch *et al.* 1984, Seal *et al.* 1987, 1988, Lentz *et al.* 2002a). As stated previously, the close spatial and temporal relationship of the Au–W–Mo mineralization to the granodiorite, along with high temperatures of deposition associated with quartz and ore minerals obtained from fluid-inclusion data in Type-I and -III mineralization (Scratch *et al.* 1984, Seal *et al.* 1987), which are similar to the fluids trapped by quartz phenocrysts within the granodiorite presented in this study (Fig. 11), support a magmatic–hydrothermal source (arrows 1 and 2 in Fig. 12) even though low-temperature and low-salinity fluids indicate a contri-

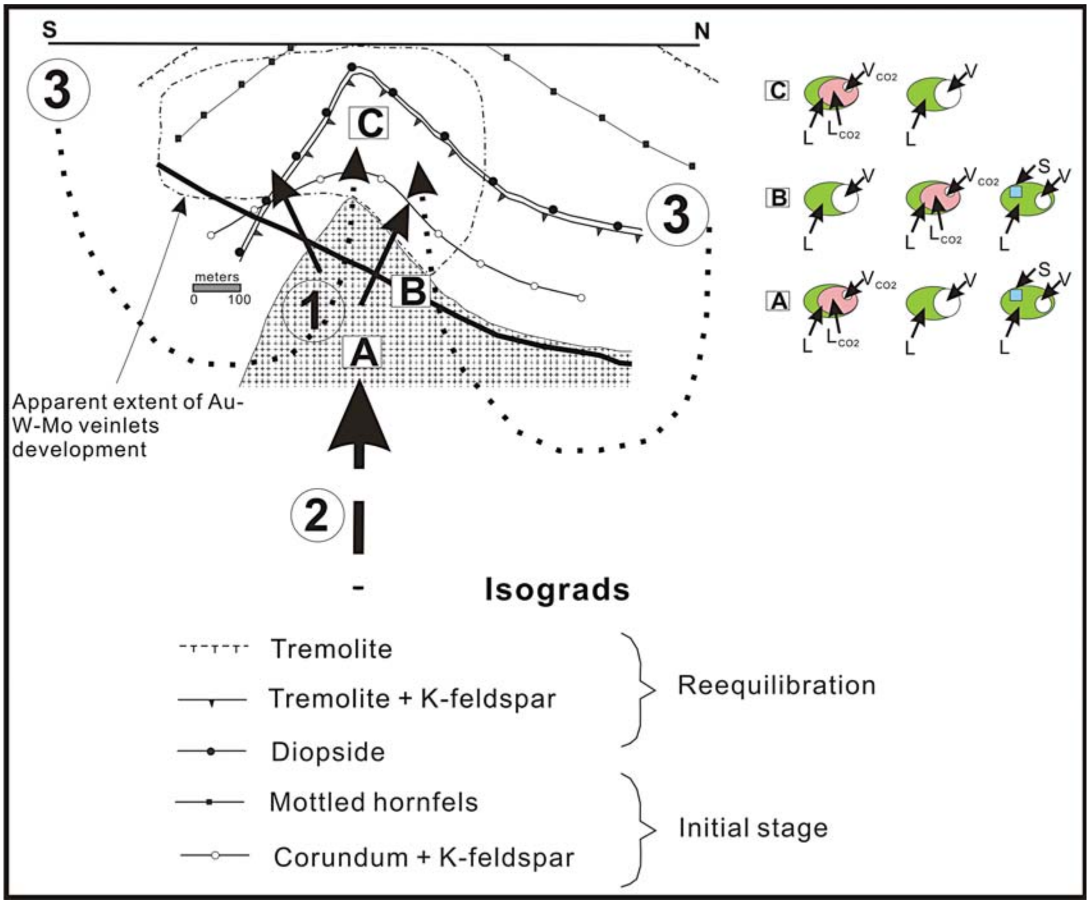

FIG. 12. A model for hydrothermal systems that interacted with the Lake George granodiorite stock and related Au–W–Mo–Sb mineralization. 1) Solid arrow: magmatic hydrothermal fluids; 2) dash arrow: Fluids derived from cooling magmas at depth; 3) dotted arrow: circulation of groundwater. A) The Lake George granodiorite stock; three types of inclusions occur: CO_2-bearing, H_2O-rich aqueous, and halite-bearing fluid inclusions. B) The Hibbard Sb ore vein; three types of inclusions occur: CO_2-bearing, H_2O-rich aqueous, and halite-bearing fluid inclusions. C) Apparent extent of development of Au–W–Mo veinlets and stockwork (Seal *et al*. 1987, Procyshyn & Morrissy 1990, Morrissy 1991a, b); two types of inclusions occur: CO_2-bearing, and H_2O-rich aqueous fluid inclusions. Location of N–S cross-section is shown in Figure 1b; the isograds were modified from Seal *et al.* (1987) and Procyshyn & Morrissy (1990).

bution from circulation of groundwater (arrow 3 in Fig. 12). Oxygen and hydrogen isotope data support this speculation.

CO_2-bearing fluids are characteristic of intrusion-related gold systems, representing deeper levels magmatic–hydrothermal ore systems (Lang & Baker 2001, Baker 2002), but the role of CO_2 in gold mineralization is not well understood. CO_2 is likely to act as a fugitive agent in hydrothermal systems, leading to unmixing of the fluids to create a separate vapor phase, owing to its very low solubility in both melts and fluids (Lowenstern 2001). This process may give rise to metal fractionation between coexisting brine and vapor phases (Heinrich *et al.* 1999, Rowins 2000, Ulrich *et al.* 2002); Au, As, and Cu preferentially partition into the vapor phase, whereas Na, K, Fe, Mn, Zn, Rb, Cs, Ag, Sn, and Pb partition into the brine. Hence, gold mineralization distal from the intrusion warrants attention during exploration.

On the basis of a thermodynamic analysis of gold solubility in magmatic fluids (Gammons & Williams-Jones 1997) and the fluid-inclusion data presented in this and previous studies, $AuCl_2^-$ is probably the dominant species in the ore fluids at higher temperatures (>500°C), and it gradually changes to $Au(HS)_2^-$ as temperature decreases (<400°C), because H_2S abundance is high and acid neutralization results from granodiorite and host-rock reactions. Phase separation of CO_2-bearing fluids with an associated increase in pH effectively extracts sulfur from the fluids as H_2S, which is preferentially partitioned into the gas phase; influx of groundwater with an associated drop in temperature may have resulted in Au deposition mainly in the exocontact aureoles adjacent to the granodiorite stock (Fig. 12).

CONCLUSIONS

A few conclusions can be made as follows, on the basis of the present fluid-inclusion and stable isotope study of the Lake George granodiorite, and a comparison with previous fluid-inclusion studies on the exocontact W–Mo mineralization (Seal *et al.* 1987) and Au-bearing antimony veins (Scratch *et al.* 1984, Seal *et al.* 1988).

1. Multiple generations of fluids in the system H_2O–NaCl–CO_2–CH_4 interacted with the Lake George granodiorite; saline aqueous fluids are subordinate. These fluids, containing appreciable Ca–Fe–K–Mg–Mn, caused partial re-equilibration and recrystallization of rock-forming minerals in the granodiorite.

2. There are similarities among the fluid inclusions in granodiorite and Au–W–Mo quartz–carbonate veinlets and stockworks, and the major Sb-bearing veins, suggesting that they may have related sources. These fluids were mainly derived from progressive exsolution of volatiles from the downward cooling magmas, although the intrusion may assimilate volatiles (CO_2–CH_4) from wallrock through hybridization, which may play an important part in redox nature of the granodiorite. The complexity of fluid inclusions recorded in phenocrystic quartz from a high level granodiorite intrusion may be an important indicator of a high potential for gold mineralization.

3. Fluid composition and T–P characteristics in the Lake George granodiorite and associated W–Mo–Au and Au–Sb deposits share similarities to those of the recently recognized type of intrusion-related gold systems. However, the preliminary microthermometric study of fluid inclusions is only the first step toward understanding fluid compositions and T–P conditions. The oxygen and hydrogen isotope data of the rock-forming minerals help constrain the sources of the fluids that reacted with the granodiorite, and test equilibrium relationship among the minerals. Detailed micro-analyses of fluid inclusions (*e.g.,* laser-Raman, PIXE and LA–ICP–MS) are warranted for a better understanding of the hydrothermal system.

ACKNOWLEDGEMENTS

We thank Mr. M.J. McLeod (New Brunswick Department of Natural Resources and Energy) for discussion on local geology and for information on zircon U–Pb dating of the Lake George granodiorite stock. Dr. Daniel J. Kontak (Nova Scotia Department of Natural Resources) generously provided help in the fluid-inclusion investigation. Dr. Douglas C. Hall (Electron Microscopy Unit, UNB) is thanked for help in SEM analysis. Oxygen and hydrogen isotopic analyses were carried out by Kerry Klassen in the isotope lab at Queen's University, which is supported by NSERC Discovery and MFA grants, Canadian Foundation for Innovation grants and the Ontario Innovation Fund. Mr. Wayne Marshall (Apocan mine manager at Lake George Mine) kindly allowed us access to the drill core and the geological information on site. The manuscript benefitted greatly from constructive comments and suggestions by Drs. Robert Seal (U.S. Geological Survey, Reston) and Daniel J. Kontak. Critical comments by reviewers Drs. Rob Linnen and Dan Marshall resulted in substantial improvement of this paper. This research is funded by a Geological Survey of Canada – Targeted Geoscience Initiative program (GSC–TGI, 010008), and a NSERC Discovery grant to D. R. Lentz, with partial support from the New Brunswick Department of Natural Resources and Energy, Freewest Resources Canada Inc., and the University of New Brunswick.

REFERENCES

BAKER, T. (2002): Emplacement depth and carbon dioxide-rich fluid inclusions in intrusion-related gold deposits. *Econ. Geol.* **97**, 1111-1117.

________ & LANG, J.R. (2001): Fluid inclusion characteristics of intrusion-related gold mineralization, Tombstone-Tungsten magmatic belt, Yukon Territory, Canada. *Mineral. Deposita* **36**, 563-582.

BODNAR, R.J. (2003): Introduction to aqueous-electrolyte fluid inclusions. *In* Fluid Inclusions: Analysis and Interpretation (I. Samson, A. Anderson & D. Marshall, eds.). *Mineral. Assoc. Can., Short Course Vol.* **22**, 81-100.

________ & VITYK, M.O. (1994): Interpretation of microthermometric data for H_2O–NaCl fluid inclusions. *In* Fluid Inclusions in Minerals: Methods and Applications (B. De Vivo & M.L. Frezzotti, eds.). *Short Course of the IMA Working Group, Inclusions in Minerals* (*Pontignano*). Virginia Tech, Blacksburg, Virginia (117-130).

BOTTINGA, Y. & JAVOY, M. (1975): Oxygen isotope partitioning among the minerals in igneous and metamorphic rocks. *Rev. Geophys. Space Phys.* **13**, 401-418.

BOWERS, T.S. (1991): The deposition of gold and other metals: pressure-induced fluid immiscibility and associated stable isotope signatures. *Geochim. Cosmochim. Acta* **55**, 2417-2434.

________ & HELGESON, H.C. (1983): Calculation of the thermodynamic and geochemical consequences of nonideal mixing in the system H_2O–CO_2–NaCl on phase relations in geologic systems: equation of state for H_2O–CO_2–NaCl fluids at high pressures and temperatures. *Geochim. Cosmochim. Acta* **47**, 1247-1275.

BROWN, P.E. & HAGEMANN, S.G. (1994): MacFlinCor: a computer program for fluid inclusion data reduction and manipulation. *In* Fluid Inclusions in Minerals: Methods and Applications (B. De Vivo & M.L. Frezzotti, eds.). *Short Course of the IMA Working Group, Inclusions in Minerals* (*Pontignano*). Virginia Tech, Blacksburg, Virginia (231-250).

CARON, A. (1996): Geology of the Pokiok Batholith aureole, with emphasis on the Lake George Mine, York County, New Brunswick. *N.B. Dep. Natural Resources and Energy, Minerals and Energy Division, Geosci. Rep.* **94-2**.

CHI, GUOXIANG (2002): Fluid compositions and temperature–pressure conditions of intrusion-related gold systems in southwestern New Brunswick – a fluid inclusion study. *Geol. Surv. Can., Current Res.* **2002-E14**, 1-11.

CLAYTON, R.N., O'NEIL, J.R. & MAYEDA, T.K. (1972): Oxygen isotope exchange between quartz and water. *J. Geophys. Res.* **77**, 3057-3067.

CRISS, R.E. & TAYLOR, H.P., JR. (1983): An $^{18}O/^{16}O$ and D/H study of Tertiary hydrothermal systems in the southern half of the Idaho batholith. *Geol. Soc. Am., Bull.* **94**, 640-663.

DIAMOND, L.W. (2001): Review of the systematics of CO_2 – H_2O fluid inclusions. *Lithos* **55**, 69-99.

FAN, HONG-RUI, ZHAI, MING-GUO, XIE, YI-HAN, & YANG, JIN-HUI (2003): Ore-forming fluids associated with granite-hosted gold mineralization at the Sanshandao deposit, Jiaodong gold province, China. *Mineral. Deposita* **38**, 739-750.

FRANK, M.R., CANDELA, P.A., PICCOLI, P.M. & GLASCOCK, M.D. (2002): Gold solubility, speciation, and partitioning as a function of HCl in the brine – silicate melt – metallic gold system at 800°C and 100 MPa. *Geochim. Cosmochim. Acta* **66**, 3719-3732.

FRANTZ, J.D., POPP, R.K. & HOERING, T.C. (1992): The compositional limits of fluid immiscibility in the system H_2O–NaCl–CO_2 as determined with the use of synthetic fluid inclusions in conjunction with mass spectrometry. *Chem. Geol.* **98**, 237-255.

FRIEDMAN, I. & O'NEIL, J.R. (1977): Compilation of stable isotope fractionation factors of geochemical interest. *In* Data of Geochemistry, 6th edition (M. Fleischer, ed.). *U.S. Geol. Surv., Prof. Pap.* **440-KK**.

FYFFE, L.R. & FRICKER, A. (1987): Tectonostratigraphic terrane analysis of New Brunswick. *Maritime Sediments and Atlantic Geology* **23**, 113-122.

GAMMONS, C.H. & WILLIAMS-JONES, A.E. (1997): Chemical mobility of gold in the porphyry-epithermal environment. *Econ. Geol.* **92**, 45-59.

GOLDSTEIN, R.H. & REYNOLDS, T.J. (1994): Systematics of fluid inclusions in diagenetic minerals. *SEPM* (*Society for Sedimentary Geology*) *Short Course* **31**.

GREGORY, R.T. & CRISS, R.E. (1986): Isotopic exchange in open and closed systems. *In* Stable Isotopes in High Temperature Geological Processes (J.W. Valley, H.P. Taylor Jr. & J.R. O'Neil, eds.). *Rev. Mineral.* **16**, 91-127.

GROVES, D. I., GOLDFARB, R.J., ROBERT, F. & HART, C.J.R. (2003): Gold deposits in metamorphic belts: overview of current understanding, outstanding problems, future research, exploration significance. *Econ. Geol.* **98**, 1-29.

HAYES, F.M., STERNER, S.M. & BODNAR, R.J. (1988): Synthetic fluid inclusions in natural quartz. IV. Chemical analyses of fluid inclusions by SEM/EDA: evaluation and method. *Geochim. Cosmochim. Acta* **52**, 969-977.

HEINRICH C.A., GÜNTHER, D., AUDÉTAT, A., ULRICH, T. & FRISCHKNECHT, R. (1999): Metal fractionation between magmatic brine and vapor, determined by microanalysis of fluid inclusions. *Geology* **27**, 755-758.

ISHIHARA, S. (1981): The granitoid series and mineralization. *Econ. Geol., 75th Anniv. Issue*, 458-484.

KEPPLER, H. & WYLLIE, P.J. (1991): Partitioning of Cu, Sn, Mo, W, U, and Th between melt and aqueous fluid in the systems haplogranite–H_2O–HCl and haplogranite–H_2O–HF. *Contrib. Mineral. Petrol.* **109**, 139-150.

KONTAK, D.J. (2002): Analysis of decrepitate mounds as a complement to fluid inclusion thermometric data: case studies from granitic environments in Nova Scotia and Peru. *PACROFI VIII, Abstr. Program*, 40-43.

________, ANSDELL, K., DOSTAL, J., HALTER, W., MARTIN, R. & WILLIAMS-JONES, A.E. (2001): The nature and origin of pegmatites in a fluorine-rich leucogranite, East Kemptville tin deposit, Nova Scotia, Canada. *Trans. R. Soc. Edinburgh: Earth Sci.* **92**, 173-200.

KYSER, T.K., O'HANLEY, D.S. & WICKS, F.J. (1999): The origin of fluids associated with serpentinization processes: evidence from stable-isotope compositions. *Can. Mineral.* **37**, 223-237.

LANG, J.R. & BAKER, T. (2001): Intrusion-related gold systems: the present level of understanding. *Mineral. Deposita* **36**, 477-489.

________, ________, HART, C.J. & MORTENSEN, J.K. (2000): An exploration model for intrusion-related gold systems. *Soc. Econ. Geol., Newsletter* **40**, 1-15.

LENTZ, D.R. (1996): U, Mo, and REE mineralization in late-tectonic granitic pegmatites, southwestern Grenville Province, Canada. *Ore Geol. Rev.* **11**, 197-227.

________, THORNE, K.G. & YANG, XUE-MING (2002a): Preliminary analysis of the controls on the various episodes of gold mineralization at the Lake George antimony deposit, New Brunswick. *In* Current Research 2001 (B.M.W. Carroll, ed.). *N.B. Dep. of Natural Resources and Energy Division, Mineral Resource Rep.* **02-4**, 55-79.

________, ________, ________ & ADAMS, M. (2002b): Shoshonitic lamprophyre dykes at the Lake George antimony deposit, New Brunswick: petrochemical characteristics and implications for gold mineralization. *In* Current Research 2001 (B.M.W. Carroll, ed.). *N.B. Dep. of Natural Resources and Energy Division, Mineral Resource Rep.* **02-4**, 41-54.

________, TRENHOLM, N. & ARCHIBALD, D.A. (2004): Calc-alkaline lamprophyric dykes around the Lake George antimony deposit, New Brunswick: age constraints and petrogenetic aspects. *Atlantic Geoscience Society Colloquium & 30th Annual General Meeting, Program Abstr.*, 20-21.

LINNEN, R.L. (1998): Depth of emplacement, fluid provenance and metallogeny in granitic terranes: a comparison of western Thailand with other tin belts. *Mineral. Deposita* **33**, 461-476.

LONGSTAFFE, F.J. (1982): Stable isotopes in the study of granitic pegmatites and related rocks. *In* Granitic Pegmatites in Science and Industry (P. Černý, ed.). *Mineral. Assoc. Can., Short Course Handbook* **8**, 373-404.

LOWENSTERN, J.B. (2001): Carbon dioxide in magmas and implications for hydrothermal systems. *Mineral. Deposita* **36**, 490-502.

MARSH, B.D. (1996): Solidification fronts and magmatic evolution. *Mineral. Mag.* **60**, 5-40.

MARTIN, R.F. (1988): The K-feldspar mineralogy of granites and rhyolites: a generalized case of pseudomorphism of the magmatic phase. *Rend. Soc. Ital. Mineral. Petrol.* **43**, 343-354.

MATSUHISA, Y., GOLDSMITH, J.R. & CLAYTON, R.N. (1979): Oxygen isotopic fractionation in the system quartz – albite – anorthite – water. *Geochim. Cosmochim. Acta* **43**, 1131-1140.

MCCOY, D., NEWBERRY, R.J., LAYER, P.W., DIMARCHI, J.J., BAKKE, A.A, MASTERMAN, J.S. & MINEHANE, D.L. (1997): Plutonic-related gold deposits of Interior Alaska. *Econ. Geol., Monogr.* **9**, 191-241.

MCLEOD, M.J., JOHNSON, S.C. & RUITENBERG, A.A. (1994): Geological map of the southwestern New Brunswick. *N.B. Dep. of Natural Resources and Energy, Mineral Resources, Map* **NR-5** (1:250,000).

MORRISSY, C.J. (1991a): Further characterization of drill core from the Lake George mine, York County, New Brunswick. *N.B. Dep. of Natural Resources and Energy, Mineral Resources, Open File Rep.* **91-8**.

________ (1991b): Gold assessment at the Lake George mine, York County, New Brunswick. *N.B. Dep. of Natural Resources and Energy, Mineral Resources, Open File Rep.* **91-1**.

________ & RUITENBERG, A.A. (1980): Geology of the Lake George antimony deposit southern New Brunswick. *Can. Inst. Mining Metall., Bull.* **73**(822), 79-84.

O'NEIL, J.R. & TAYLOR, H.P., JR. (1967): The oxygen isotope and cation exchange chemistry of feldspars. *Am. Mineral.* **52**, 1414-1437.

PARRY, W.T. (1986): Estimation of XCO_2, P, and fluid inclusion volume from fluid inclusion temperature measurements in the system $NaCl–CO_2–H_2O$. *Econ. Geol*. **81**, 1009-1013.

PROCYSHYN, E.L. & MORRISSY, C.J. (1990): Geology of the Lake George mine, southern New Brunswick. *In* 8th IAGOD Symposium, Field Trip Guidebook, Mineral Deposits of New Brunswick and Nova Scotia (Field trip 2) (D.R. Boyle, ed.). *Geol. Surv. Can., Open File* **2157**, 58-72.

ROEDDER, E. (1984): Fluid inclusions. *Rev. Mineral.* **12**.

ROLLINSON, H.R. (1993): *Using Geochemical Data: Evaluation, Presentation, Interpretation.* Longman Scientific and Technical, London. U.K.

ROWINS, S.M. (2000): Reduced porphyry copper–gold deposits: a new variation on an old theme. *Geology* **28**, 491-494.

SAVARD, M.M. & CHI, GUOXIANG (1998): Cation study of fluid inclusion decrepitates in the Jubilee and Gays River (Canada) Zn–Pb deposits – characterization of ore-forming brines. *Econ. Geol.* **93**, 920-931.

SCRATCH, R.B., WATSON, G.P., KERRICH, R. & HUTCHINSON, R.W. (1984): Fracture-controlled antimony–quartz mineralization, Lake George deposit, New Brunswick: mineralogy, geochemistry, alteration, and hydrothermal regimes. *Econ. Geol.* **79**, 1159-1186.

SEAL, R.R., II, CLARK, A.H. & MORRISSY, C.J. (1987): Stockwork tungsten (scheelite)-molybdenum mineralization, Lake George, southwestern New Brunswick. *Econ. Geol.* **82**, 1259-1282.

________, ________ & ________ (1988): Lake George, southwestern New Brunswick: a Silurian, multi-stage, polymetallic (Sb–W–Mo–Au–base metal) hydrothermal centre. *In* Recent Advances in the Geology of Granite-Related Mineral Deposits (R.P. Taylor & D.F. Strong, ed.). *Can. Inst. Mining Metall., Spec. Vol.* **39**, 252-264.

SHABANI, A.A.T. (1999): *Mineral Chemistry and Mössbauer Spectroscopy of Micas from Granitic Rocks of the Canadian Appalachians*. Ph.D. thesis, University of Ottawa, Ottawa. Ontario.

SHEPHERD, T.J., RANKIN, A.H. & ALDERTON, D.H.M. (1985): *A Practical Guide to Fluid Inclusion Studies*. Blackie, Glasgow, U.K.

SUZOUKI, T. & EPSTEIN, S. (1976): Hydrogen isotope fractionation between OH-bearing minerals and water. *Geochim. Cosmochim. Acta* **40**, 1229-1240.

TAYLOR, H.P., JR. (1974): The application of oxygen and hydrogen isotope studies to problems of hydrothermal alteration and ore deposition. *Econ. Geol.* **69**, 843-883.

________ (1978): Oxygen- and hydrogen-isotope studies of plutonic rocks. *Earth Planet. Sci. Lett.* **38**, 177-210.

________ (1988): Oxygen, hydrogen, and strontium isotope constraints on the origin of granites. *Trans. R. Soc. Edinburgh: Earth Sci.* **79**, 317-338.

THOMPSON, J.F.H., SILLITOE, R.H., BAKER, T., LANG, J.R. & MORTENSEN, J.K. (1999): Intrusion-related gold deposits associated with tungsten–tin provinces. *Mineral. Deposita* **34**, 323-334.

TUTTLE, O.F. & BOWEN, N.L. (1958): Origin of granite in the light of experimental studies in the system $NaAlSi_3O_8 – KAlSi_3O_8–SiO_2 – H_2O$. *Geol. Soc. Am., Mem.* **74**.

ULRICH, T., GÜNTHER, D. & HEINRICH, C.A. (2002): The evolution of a porphyry Cu–Au deposit, based on LA–ICP–MS analysis of fluid inclusions: Bajo delar Alumbrera, Argentina. *Econ. Geol.* **97**, 1889-1920.

WHALEN, J.B. (1993): Geology, petrography, and geochemistry of Appalachian granites in New Brunswick and Gaspésie, Quebec. *Geol. Surv. Can., Bull.* **436**.

________, JENNER, G.A., LONGSTAFFE, F.J. & HEGNER, E. (1996): Nature and evolution of the eastern margin of Iapetus: geochemical and isotopic constraints from Siluro-Devonian granitoid plutons in the New Brunswick Appalachians. *Can. J. Earth Sci.* **33**, 140-155.

WHITNEY, J.A. (1988): The origin of granite: the role and source of water in the evolution of granitic magmas. *Geol. Soc. Am., Bull.* **100**, 1886-1897.

WILLIAMS-JONES, A.E. & FERREIRA, D.R. (1989): Thermal metamorphism and $H_2O–CO_2$–NaCl immiscibility at Patapedia, Quebec: evidence from fluid inclusions. *Contrib. Mineral. Petrol.* **102**, 247-254.

YANG, XUE-MING, LENTZ, D.R. & CHI, GUOXIANG (2002a): Petrochemistry of Lake George granodiorite stock and related Au mineralization, York County, New Brunswick. *Geol. Surv. Can., Current Res.* **2002-D7**, 1-10.

________, ________, HALL, D.C. & CHI, GUOXIANG (2002b): Petrology of the Lake George granodiorite stock, New Brunswick: implications for crystallization conditions, volatile exsolution, and W–Mo–Au–Sb mineralization. *Geol. Surv. Can., Current Res.* **2002-E14**, 1-12.

YARDLEY, B.W.D. & LONG, C.B. (1981): Contact metamorphism and fluid movement around the Easky adamellite, Ox Mountains, Ireland. *Mineral. Mag.* **44**, 125-131.

Received January 20, 2003, revised manuscript accepted May 25, 2004.